Flight Testing Automation to Parameterize Unmanned Aircraft Dynamics

Or D. Dantsker*, Simon Yu† and Moiz Vahora‡
University of Illinois at Urbana–Champaign, Urbana, IL 61801
Marco Caccamo §
Technical University of Munich (TUM), Garching, Germany

In recent years, we have seen an uptrend in the popularity of unmanned aerial vehicles (UAVs) driven by the desire to apply these aircraft to a variety of civilian, commercial, education, government, and military applications. With the rapid increase in UAV application, significant effort has been put forth into research and development, which culminates with flight testing of the vehicle. Flight testing occurs using either a partial-scale or a full-scale prototype and includes a series of maneuvers used to measure and verify the aircraft's aerodynamics and control behavior. Most often, UAVs are manually piloted through at least the initial flight testing stage where flight qualities are recorded and translated into control tuning. This paper describes a flight testing automation process to streamline the parameterization of an unmanned aircraft's flight dynamics. The developed flight testing automator commands the aircraft through a predetermined, conditional set of motions and states to induce certain maneuver sets, which allow for dynamics to more easily be parameterized. The desired maneuver sets follow the standards and generally accepted practices for full-scale flight testing. Specifically, the maneuvers of interest presented in this paper include: idle descent, stall, phugoid, doublets, and singlets, which provide the basis for determining the aircraft aerodynamics, longitudinal stability, and control effectiveness, respectively. The flight testing automator was implemented and demonstrated using software-in-the-loop simulation, including a comparison with manually-piloted flight, followed by flight testing using a fixed-wing trainer-type UAV. Automating the data collection process, as opposed to the previous status quo of manual piloting, would allow for more efficient aircraft parametrization and modelling by minimizing trial-and-error and, more importantly, reducing the flight time required.

Nomenclature

PID	=	proportional–integral–derivative	V_S	=	stall speed
UAV	=	unmanned aerial vehicle	x, y, z	=	position in ENU coordinate system
a_x, a_y, a_z	=	body-axis translational acceleration	α	=	angle-of-attack
p, q, r	=	roll, pitch and yaw rotation rates	β	=	sideslip angle
u, v, w	=	body-fixed true velocity	ϕ, θ, ψ	=	roll, pitch and heading angles
V	=	total speed			

*Ph.D. Student, Department of Aerospace Engineering, AIAA Student Member. dantske1@illinois.edu
†M.S. Student, Department of Electrical and Computer Engineering. jundayu2@illinois.edu
‡M.S. Student, Department of Aerospace Engineering, AIAA Student Member. mvahor2@illinois.edu
§Professor, Department of Mechanical Engineering. mcaccamo@tum.de

I. Introduction

In recent years, we have seen an uptrend in the popularity of unmanned aerial vehicles (UAVs) driven by the desire to apply these aircraft to areas such as precision farming, infrastructure and environment monitoring, surveillance, surveying and mapping, search and rescue missions, weather forecasting, and more. With the rapid increase in UAV application, significant effort has been put forth into research and development, which culminates with flight testing of the vehicle. Flight testing occurs using either a partial-scale or full-scale prototype and includes a series of maneuvers, which will measure and verify the aircraft's aerodynamics and control behavior. For example, significant effort has been put into studying the aerodynamic qualities of UAVs,[1,2] especially in high angle-of- attack conditions,[3–5] as well as the development of new control algorithms.[6–10] In addition, unmanned aircraft are often used as low-cost stand-ins for experiments that are too risky or costly to perform on their full-scale counterparts.[11–13] They are often also used to explore new aircraft configurations[14–17] or flight hardware.[18–20] Most often, these UAVs are either manually-piloted for the entirety of flight testing or for the initial flight testing stage (during which their flight qualities are recorded, translated into control tuning, and only then are flown autonomously).

This paper describes a flight testing automation process to streamline the parameterization of an unmanned aircraft's flight dynamics. The developed flight automator commands the aircraft through a predetermined, conditional set of motions and states to induce certain maneuver sets, which allow for aircraft to more easily be parameterized in post-processing. The desired maneuver sets follow the standards and generally accepted practices for full-scale flight testing, as outlined by Kimberlin.[21] Specifically, the maneuvers of interest presented in this paper include: idle descent, stall, phugoid, doublets, and singlets; which provide the basis for determining the aircraft aerodynamics, longitudinal stability, and control effectiveness, respectively. The flight testing automator, which extends previous works,[22–25] was initially implemented and demonstrated using software-in-the-loop simulation. The flight automator was integrated into the open source uavAP autopilot,[26,27] which commanded a full-scale Cessna 172 in X-Plane 11 Flight Simulator;[28] the open-source uavEE emulation environment provided the necessary interface infrastructure.[29,30] After the flight automator demonstrated the maneuvers of interest, a comparison was made between flight test automation and manually-pilot controlled flight testing; specifically, an automated stall maneuver was compared to a manually-piloted stall maneuver. Finally, a flight testing demonstration was performed using a fixed-wing trainer-type UAV for a subset of maneuvers.

Automating the data collection process, as opposed to the previous status quo of manual piloting of UAVs through certain maneuvers to collect flight data ,[2–4,12,13,16,31,32] allows for the aircraft parametrization, and thus the modeling process, to be performed with minimal trial-and-error, which more importantly, reduces the flight time required. For example, by automating the flight testing process, aircraft inertial state variables such as Euler angles, rotation rates, and velocities can be set and maintained during flight, with greater accuracy, than with manual piloting. It is important to note that performing consistent maneuvers with UAVs is difficult in comparison to manned aircraft as the UAV needs to be observed from the sideline of the runway rather than from inside of the aircraft (or from a ground control station). UAV pilots are often relatively far away, and cannot easily observe aircraft attitude and velocities without relying on telemetry and/or an assistant to receive such information. Additionally, given generally accepted flight testing practices and current regulations, it is necessary to maintain the aircraft within line-of-sight. Most often, a desired flight testing maneuver is performed, centered in front of the pilot, which limits the effective maneuvering box and may often be very difficult.[5,11,23,24,31] With the use of the flight test automator, an aircraft can easily be maneuvered to the edge of the safety pilot's vision boundary, and once reoriented towards the center, the maneuver set can be initiated, allowing for the largest allowable experiment area.

This paper will first discuss the development of flight testing automation including how maneuvers are performed and how internal condition based transitions are made. Then, flight testing automation will be implemented and demonstrated in simulation. A comparison between a stall maneuver performed manually by a human pilot versus on performed autonomously will be made. This will be followed by a demonstration with actual flight testing. Finally, a summary and statement of future work will be given at the end of the paper.

II. Development

The flight testing automation process was developed to streamline the parameterization of an unmanned aircraft's flight dynamics. Specifically, the flight test automator was designed such that it could command an aircraft through a set of predetermined maneuvers and allow for straightforward determination of aircraft parameters. The aim was to develop a routine which could be performed by a basic proportional-integral-derivative (PID) flight controller that has had very basic tuning. The maneuvers integrated into the flight testing automator were adapted from standards and generally accepted practices for full-scale flight testing, as outlined by Kimberlin.[21] The maneuvers of interest are idle descent, stall, phugoid, doublets, and singlets. These maneuvers have long been used for parameterization of aircraft aerodynamics, longitudinal stability, and control effectiveness, respectively. In the following sub-sections we describe how each maneuver is performed and the conditions by which transitions are made between the sub-elements of a maneuver.

A. Flight Maneuvers

1. Trim Analysis

Trim analysis is performed in order to determine the trim state for each of the control surfaces for a given flight condition. Unlike manually-pilot flight where the pilot trims the aircraft to a given flight condition, an autonomously-piloted aircraft is controlled with the use of PID where the center setting is semi-arbitrarily set (e.g. the physical geometric center angle) and the effective trim is maintained by the integral term. However, in many cases, knowledge of effective trim position is desired so that the control surfaces can be returned to trim center upon command. For example, after an excitation (singlet or doublet) it is desired that the control surfaces be returned to trim such that the un-actuated response can be recorded.

Therefore, in order to determine the trim of the aircraft, the aircraft is commanded to fly in a certain flight condition, e.g. steady level flight at $1.5V_S$ (1.5 times the stall speed). Once the aircraft has reached steady state, i.e. as defined by the maneuver parameters (with Euler angles and rotation rates maintained within given noise limits for a prescribed amount of time), the aircraft controls are recorded and then averaged over a certain period of time. The resulting values are considered as trims for that tested flight condition. It should be noted that this maneuver requires low environmental disturbances (e.g. wind, thermals, etc).

2. Stall Speed

Knowledge of the stall speed for an aircraft is fundamentally necessary for basic aircraft operation as well as performing other flight testing maneuvers. In order to determine stall speed, we apply the flight testing method described in the literature for full-scale aircraft,[21] as it is applicable to smaller aircraft as well. The stall speed maneuver is conducted starting at sufficient altitude for the expected altitude loss with the aircraft flying in steady level flight. The aircraft propulsion system is then powered off with the flight automator commanded to maintain the starting altitude. For the stall speed maneuver, the ailerons are actuated to maintain 0 deg roll. Gradually as the aircraft slows, it increases the up elevator deflection. As this occurs the angle of attack increases up until the point where the aircraft stalls, causing the nose to drop. The nose drop is detected by monitoring the pitch rate, e.g. when it exceeds 15 deg/s for the simulated Cessna 172. This can occur in 2 ways: the nose will drop before maximum elevator deflection is reached or the nose will drop after the elevator has reached full deflection and it is no longer able to maintain altitude.

Once stall is detected, the flight automator recovers from the stall by centering the control surfaces to trim positions (as analyzed earlier) and waits until sufficient velocity is reached. Often the flight automator is also set to recover at a given 'safety floor' altitude. Once either of these conditions are met, power is applied to the propulsion system and the aircraft pulls up and out of the descent. It should be noted that upset scenarios may occur, e.g. spin, that require external, safety pilot, assistance to recover from.

3. *Stall Polar*

Determining the lift, drag, and moment curves for an aircraft provides a researcher or developer a great deal of information, e.g. aircraft performance polars, best climb rate or glide angle, etc. A stall polar maneuver was developed in which an aircraft is placed in a un-powered, trimmed climb, which is followed by a gradual sweep of angle-of-attack. This maneuver effectively sweeps the un-actuated aircraft through a range of angle-of-attacks, up to stall and back down through the recovery, showing possible hysteresis.

The stall polar maneuver begins with steady level flight at a sufficient altitude, e.g. 200m for a full-scale Cessna 172 (in simulation). The throttle is then cut with roll being maintained to 0 deg. Then the aircraft pitches down to -30 deg, and after descending, e.g. to 200 m, the aircraft pitches up 30 deg at which point the elevator is centered to trim. The aircraft is allowed to continue unaided while it decelerates and sweeps through a range of angle-of-attacks as it pitches down. Depending on the setup up and parameters used, i.e. initial altitude drop and pitch up angle, different max angle of attacks can be reached. Once the aircraft pitches back down to -30 deg, a powered recovery is initiated.

4. *Phugoid*

Elevator induced phugoids are used to characterize the longitudinal stability of the aircraft as it settles back into the trim configuration. The motion of small to medium class UAVs differ from larger aircraft through the time response of the maneuver, as the settling time is inversely proportional to the size to the aircraft. As small to medium class UAVs require less time to settle and have higher oscillation frequencies, high-frequency data acquisition is necessary to precisely record the maneuver characteristics.

The flight test procedure for the phugoid maneuver was developed using a similar methodology for full-scale aircraft as outlined in Kimberlin. The test begins with the aircraft at a sufficiently high altitude such that the rest of the maneuver can safely occur, e.g. 300 m for a full-scale Cessna 172 (in simulation). The throttle is then cut and the roll of the aircraft is maintained to 0 deg. The aircraft is pitched down to -30 deg and after descending, e.g. to 200 m, the aircraft is pitched up 20 deg and the elevator is centered to trim as it enters into the phugoid. The phugoid mode is allowed to proceed until the aircraft reaches a 'safety floor' altitude, e.g. 100 m, at which point the throttle is re-engaged and the aircraft is recovered from the maneuver. There are two variants of this maneuver, where the ailerons are either locked in the trim position or are controlled to maintain 0 deg roll angle; the latter option guarantees that the aircraft tracks straight with moderate environmental disturbances.

5. *Idle Descent*

The idle descent maneuver is used to determine the glide characteristics of an aircraft, total drag acting upon it, and the aircraft neutral point. This maneuver begins with the aircraft in its trimmed configuration at a sufficiently high altitude, after which the throttle is cut, and the automator pitches the aircraft down to an estimated glideslope then commands the elevator into a desired trimmed setting. During this whole sequence, 0 deg roll is actively maintained using the ailerons.[21] The aircraft then proceeds to glide until it reaches its cutoff 'safety floor' altitude, at which point it is recovered similarly to other maneuvers.

6. *Doublet and Singlets*

Doublet and singlets, also known as the short period maneuver, are used to characterize longitudinal stability and characteristics of an aircraft through a critically damped oscillation. This maneuver can be used to evaluate control surface effectiveness and determine control surface coefficients. Singlet and doublet excitations are executed using a pulse input on the control surface of interest using the flight automator. This maneuver is executed starting at a sufficient altitude and a prescribed velocity, often at $1.5V_S$. After the aircraft reaches a steady state, the throttle command is locked to maintain fixed speed and the roll and pitch target angles are set to 0 deg; at this point, the control surface positions are recorded as relative trim. The automator then performs the singlet or doublet maneuver by deflecting the

control surface using a square impulse wave¿ After the square wave concludes, all control surfaces are locked to their trim positions for a given time, allowing the aircraft motion to settle. Once this ends, the aircraft is recovered.

B. Maneuver Conditional Transitions

As described in the previous section, maneuvers are made up of several sub-maneuvers which occur progressively as certain condition criteria are met.The transitions between these sub-maneuvers, i.e. functional steps within a maneuver, occur conditionally in one of three ways: a time-based condition, a steady state condition, or a sensor data condition.

The simplest of the transitions is time-based: once a prescribed amount of time has passed, the maneuver will transition from one sub-maneuver to the next sub-maneuver. An example of a time-based transition condition are the control surface excitations for the singlets or doublets; specifically, once the control pulse is started, it will be maintained for a given period of time before it concludes and the maneuver continues to the following step.

The next transition is steady state, that is that the maneuver will proceed once a given state has remained within a defined threshold for a given period of time. An example of this is the trim analysis whereas the automator waits until the aircraft has reached a steady state before beginning to record the average control surface trim values. Steady state conditions require either minimal or constant environmental effects such that the aircraft remains undisturbed in its current state.

The final type of transition is sensor data, whereby the automator waits until a single or multiple sensor data values meet or exceed prescribed targets. An example of this is the stall speed maneuver, whereby the automator waits for a negative (nose downward) pitch rate before recognizing stall and commanding the elevator to trim deflection.

By combining the three types of conditional transitions, a great variety of maneuvers can be formed. This process allows a user to convert manual flight testing techniques into automated maneuver sets which can greatly hasten flight testing. Not only can flight testing maneuvers be performed more exact with conditional based transitions, but also, doing so allows these maneuvers to be done so with excellent repeatability.

III. Simulation

The flight testing automator was implemented and demonstrated using software-in-the-loop simulation. After simulation had been performed for all of the desired maneuvers, a comparison was made between a manually-controlled maneuver and its autonomous counterpart.

A. Setup

The setup for the simulations of the flight testing maneuvers is shown in Figure 1. The flight testing automator which was custom integrated into the open source uavAP autopilot[27] by means of a flexible flight maneuver automation framework.[33] A highly-accurate dynamics model of a Cessna 172 was simulated by the X-Plane 11 Flight Simulator, which was interfaced with uavAP via the uavEE emulation environment.[29,30] uavEE allowed for efficient and reliable sensing and actuation to travel between the autopilot and the flight simulator. Additionally, it also provided real-time flight monitoring through a ground station user interface.

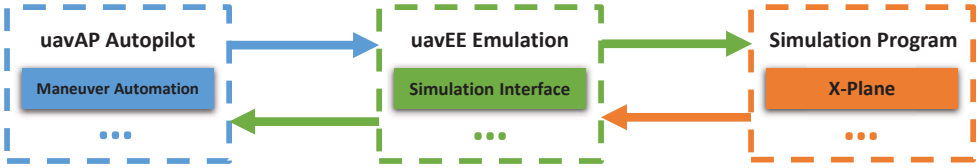

Figure 1: The simulation setup where uavAP autopilot, which integrated the flight testing automator, is interfaced with X-Plane 11 Flight Simulator through the uavEE emulation environment.

B. Maneuver Examples

The maneuvers presented in Section II.A were implemented into the flight automator and demonstrated using the X-Plane 11 Flight Simulator. The specific parameters (velocities, altitudes, and condition cutoffs), were adapted to the aircraft dynamics (flight velocity, inertia) of the simulated full-scale Cessna 172. Trajectory plots and time histories of these maneuvers are provided in Appendix A.

C. Automated vs Manually-Piloted Comparison

In order to demonstrate the effectiveness of automating flight testing maneuvers, a stall speed maneuver was flown using the full-scale Cessna 172 in the X-Plane 11 Flight Simulator, both manually and autonomously, and then compared. The manually-pilot aircraft was flown by a human pilot using a professional-grade simulator yoke system, throttle quadrant, and rudder pedals. Both maneuvers were set up the same with the aircraft flying at 40 m/s and oriented at a heading of 0 deg (East).

Before the executions of both automated and manual maneuver set, the control trim surfaces of the Cessna were trimmed such that all the primary controls are centered with zero input, i.e. the aircraft trims were set identically. In the automated maneuver set, the trim of the aircraft is automatically analyzed and applied by the trim analysis. In the manual maneuver set, the trim is performed by adjusting the trim configuration of the X-Plane 11 using the digital joystick. The executions of both of the maneuver sets were recorded.

The results of both the manually-operated and automated stall speed maneuver are presented in Figs. 3–6. From the time histories, it can be seen that the magnitude of the pitch rate of the aircraft is small or close to zero for the majority of the flight with a noticeable spike around 24 to 26 sec for both maneuver sets, correlating the nose drop associated with a stall. During that time interval, the aircraft stall speed for both maneuvers was observed as approximately 26 to 27 m/s.

The manually operated stall maneuver shows signs of variations and oscillations throughout the data, particularly in the time history of the accelerations, rotation rates, Euler angles, and angle-of-attack. As expected, the manually-commanded control is not smooth, which caused the aforementioned disturbances. These features point towards the difficulty exhibited by the human pilot, in manually controlling the aircraft altitude and roll and heading angles, simultaneously. In comparison, the time history of autonomously controlled stall speed maneuver show smooth and accurate results. It is also expected that the autonomous stall speed maneuver is very repeatable in comparison to the maneuver, which was manually-piloted.

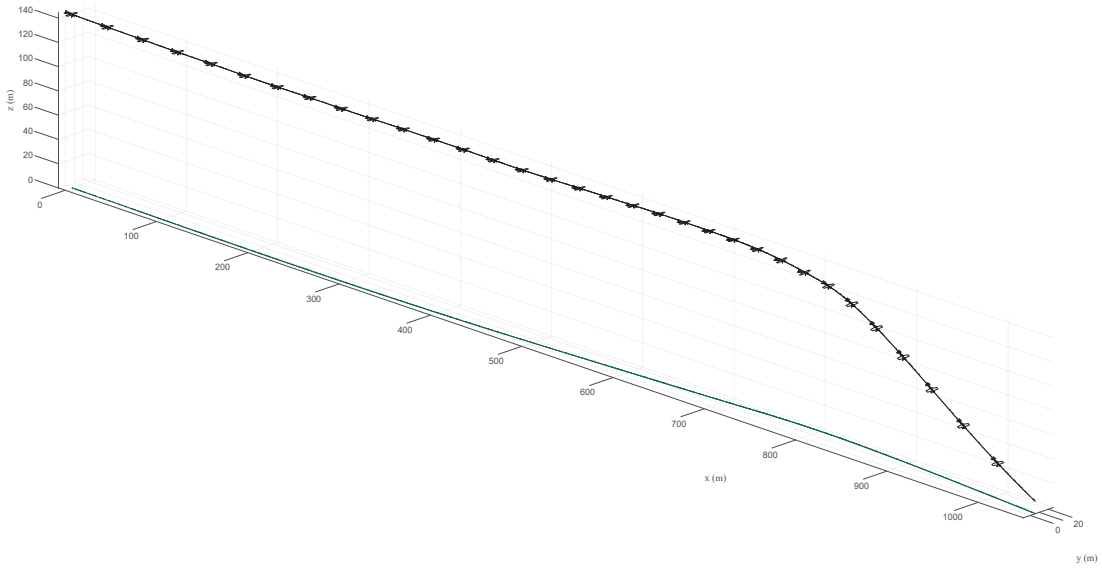

Figure 2: Trajectory plot of a stall speed maneuver performed by manual piloting (the aircraft is drawn once every 1.0 s).

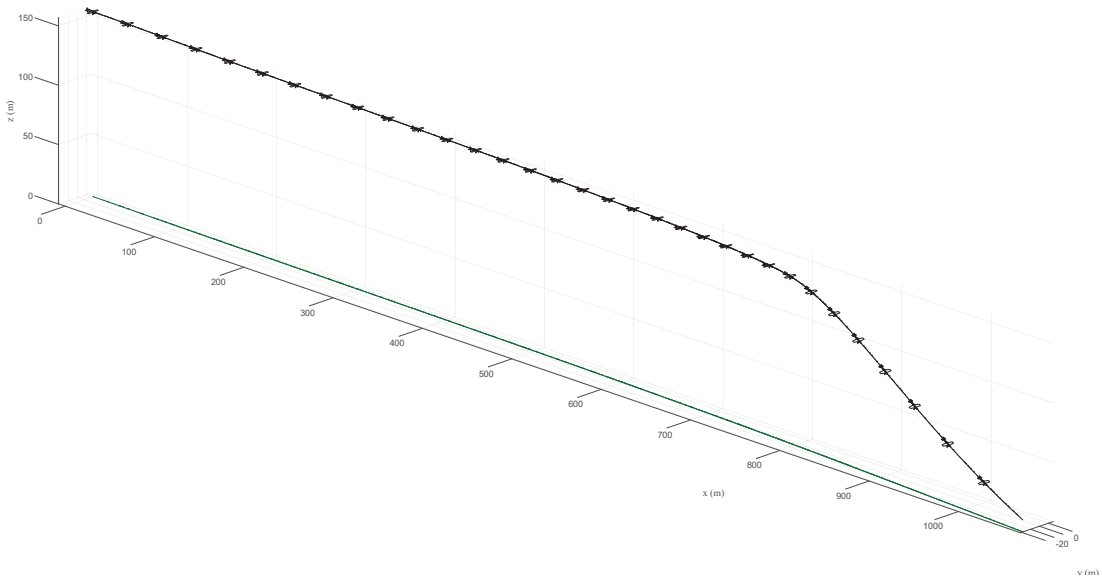

Figure 3: Trajectory plot of a stall speed maneuver performed by the maneuver automator (the aircraft is drawn once every 1.0 s).

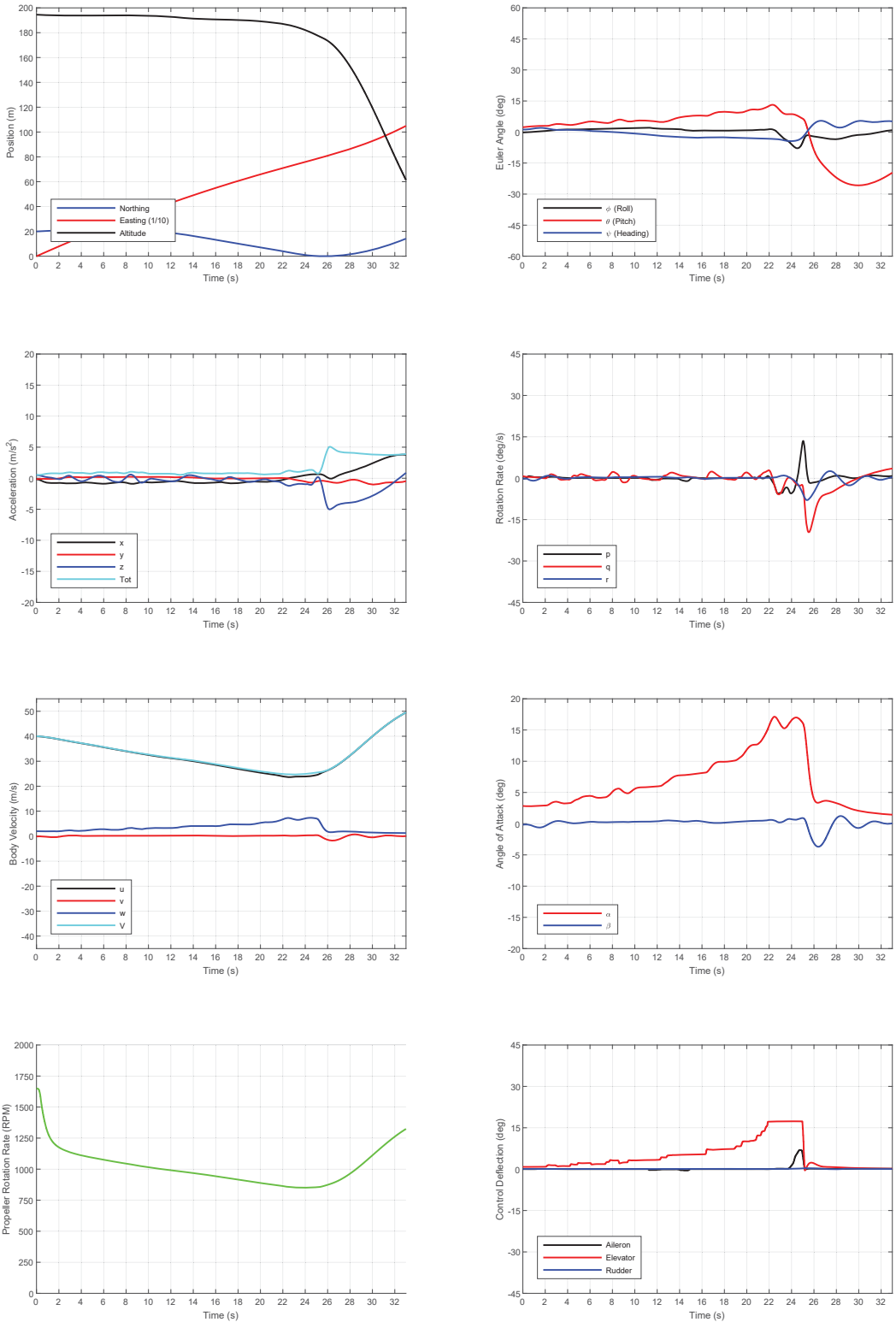

Figure 4: A time history of a stall speed maneuver performed by manual piloting.

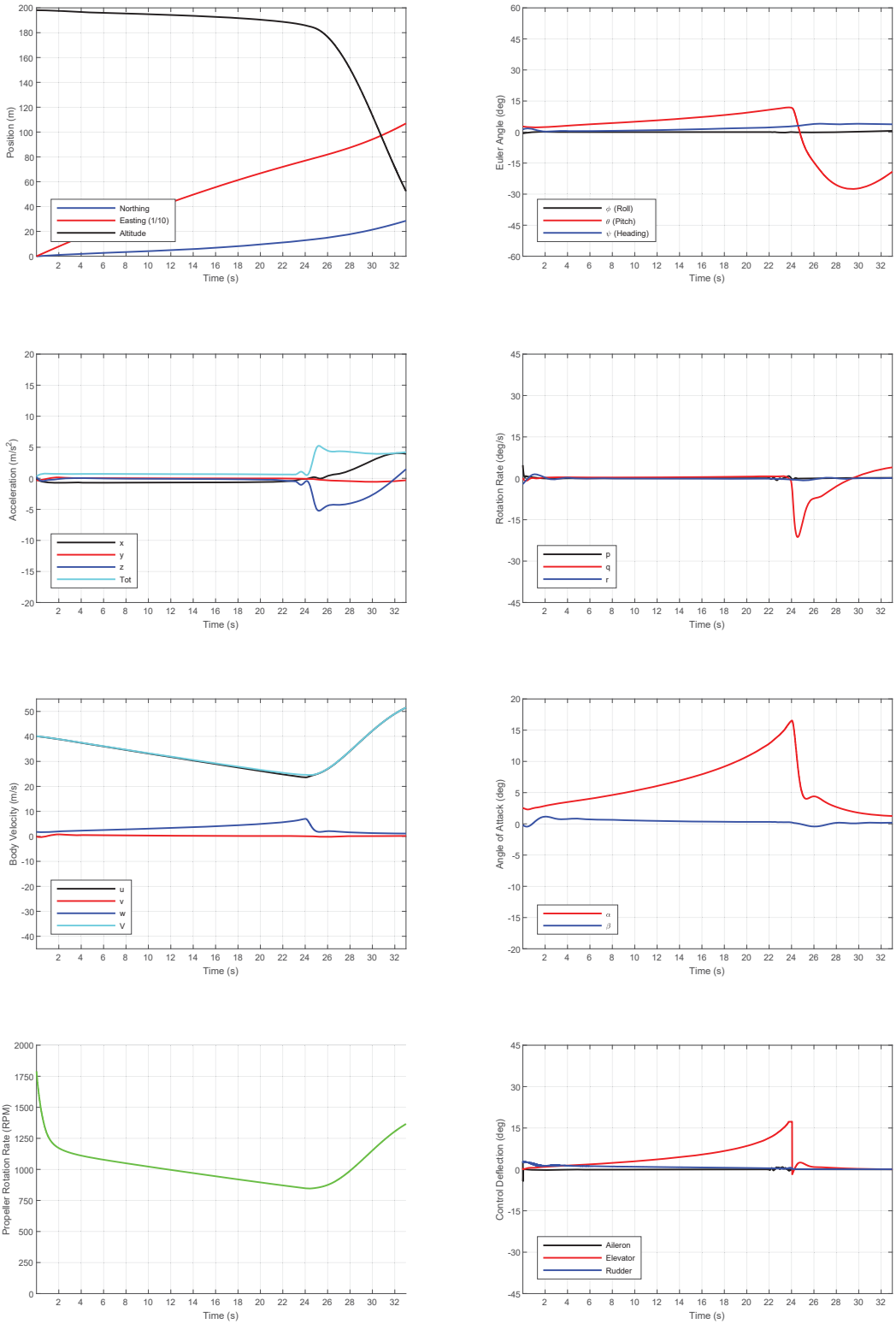

Figure 5: A time history of a stall speed maneuver performed by the maneuver automator.

IV. Flight Testing

The flight testing automator was demonstrated using an existing aircraft, the Avistar UAV, which was previously used for avionics development[34–36] as well as power modelling[37] and emulation environment demonstration.[29] The aircraft was flown through a subset of the maneuvers presented in Section II using the flight testing automator.

A. Aircraft Setup

The Avistar UAV aircraft was developed off of the Great Planes Avistar Elite fixed-wing trainer-type radio control model and has a wingspan of 1.59 m and a mass of 3.92 kg. The completed flight-ready aircraft is shown in Figure 6 and its physical specification are given in Table 1. Component specifications can be found in.[35]

The aircraft was instrumented with an Al Volo FC+DAQ flight computer and data acquisition system,[38] which incorporates the open source uavAP autopilot. The specifications of the instrumentation used for flight testing are given in Table 2. Further detail regarding the open source uavAP autopilot can be found in related literature.[26,29] The complete physical, component, and instrumentation specifications can be found in.[37]

Figure 6: Flight-ready Avistar UAV.

Table 1: Avistar UAV aircraft physical specifications.

Geometric Properties	
Overall Length	1395 mm (55.0 in)
Wing Span	1590 mm (62.5 in)
Wing Area	43.3 dm^2 (672 in^2)
Aspect Ratio	6.62
Inertial Properties	
Mass/Weight	
Empty (w/o Battery)	3.39 kg (7.46 lb)
4S LiPo Battery	0.53 kg (1.17 lb)
Gross Weight	3.92 kg (8.63 lb)
Wing Loading	90.5 gr/dm^2 (29.6 oz/ft^2)

Table 2: The instrumentation on the Avistart UAV.

Instrumentation system	Al Volo FC+DAQ 400 Hz system
Sensors	
Inertial	XSens MTi-G-700 AHRS with GPS
Airspeed	Al Volo pitot-static airspeed sensor
Motor Sensors	Al Volo Castle ESC sensor
Power	
Regulator	Built into FDAQ
Battery	Thunder Power ProLite 3S 1350 mAh

B. Maneuver Examples

The Avistar UAV was flight tested in the spring of 2019 using the flight testing automator. Due to limited calm weather opportunities, only a subset of possible maneuvers were demonstrated. These include stall speed, stall polar, idle descent, and roll doublet. Trajectory plots and time histories of these maneuvers are provided in Appendix B.

The trajectory and time history of the stall speed maneuver are shown in Figs. 31 and 32. As can be seen in the time history plot, the aircraft starts off approximately level with power to the propeller being reduced. As the aircraft slows down, it gradually applies more elevator and pitches up until it reaches stall at 6.0 s. The stall speed observed is approximately 14 m/s. Once the aircraft stall, all the controls are returned to trim state.

Figs. 33 and 34 show the trajectory and time history of the stall polar maneuver being performed. The flight testing automator initiates the maneuver by cutting power to the propeller, pitching down 30 deg and descending 50 m, then pitching up to 30 deg, and centering the controls to their trim positions. The aircraft then decelerates and sweeps through a range of 0 to 15 to 0 deg of angle-of-attack as it pitches down. During this final part of the maneuver, there is minimal, i.e. less than 5 deg, of side-slip indicating that the motion is mostly in the longitudinal direction.

In Figs. 35 and 36, an idle descent is presented. The maneuver is relatively simple with the flight testing automator pitching the aircraft down to approximately -15 deg, then centering the elevator to trim position. Note that the aileron is used during the maneuver to keep the aircraft level, which is consistent with the advice given by Kimberlin.

The trajectory and time history of the roll and pitch doublet maneuvers are shown in Figs. 37 and 38 and Figs. 39 and 40, respectively. Both maneuvers start with the aircraft flying relatively level with power applied to the propeller to keep the velocity at approximately 20 m/s. Then a set of square waves (positive then negative) are sent to the ailerons and elevators, respectively, while the other control surfaces are locked at their trim positions. All of the control surfaces are then maintained at their trim positions allowing the aircraft to naturally dampen. As expected, there is some coupling between the roll and yaw axes during the roll doublet. It should be noted that for future testing, both the period and amplitude of each of the square waves will be adjusted iteratively to generate the desired response for each axis.

V. Summary and Future Work

This paper describes a flight testing automation process that was demonstrated to streamline flight testing and can parameterize the flight dynamics of an unmanned aircraft. The developed flight testing automator commands the aircraft through a predetermined, conditional set of motions and states to induce certain maneuver sets, which would allow for dynamics to more easily be parameterized. The maneuvers of interest presented in this paper include: idle descent, stall, phugoid, doublets, and singlets, which provide the basis for determining the aircraft aerodynamics, longitudinal stability, and control effectiveness, respectively. The flight testing automator was implemented and demonstrated using software-in-the-loop simulation; a comparison with manually-piloted flight was also performed for testing stall, demonstrating the advantage of the automator. The flight testing automator was then demonstrated through actual flight testing using a fixed-wing trainer-type unmanned aircraft. Automating the data collection process, as opposed to the previous status quo of manual piloting, allows for more efficient flight testing by minimizing trial-and-error and, more importantly, decreases the flight time required.

In future work, the flight testing automator will be expanded to perform additional maneuvers as well as sweeping the parameters of maneuvers during a flight testing session. There is currently interest in supporting such maneuvers as accelerated stalls, i.e. stalls occurring during high-g turns, and spins. For maneuvers such as singlets and doublets, the automator will be able able to support a range sweep for square wave periods and amplitudes. Additionally, further flight testing is planned to demonstrate the real-life repeatability of the flight automation process; further comparison to manually-piloted flight will also be performed. Additionally, there is interest in applying the flight testing automator to additional aircraft projects.

Appendix A: Simulator Testing Results

A. Trim Analysis

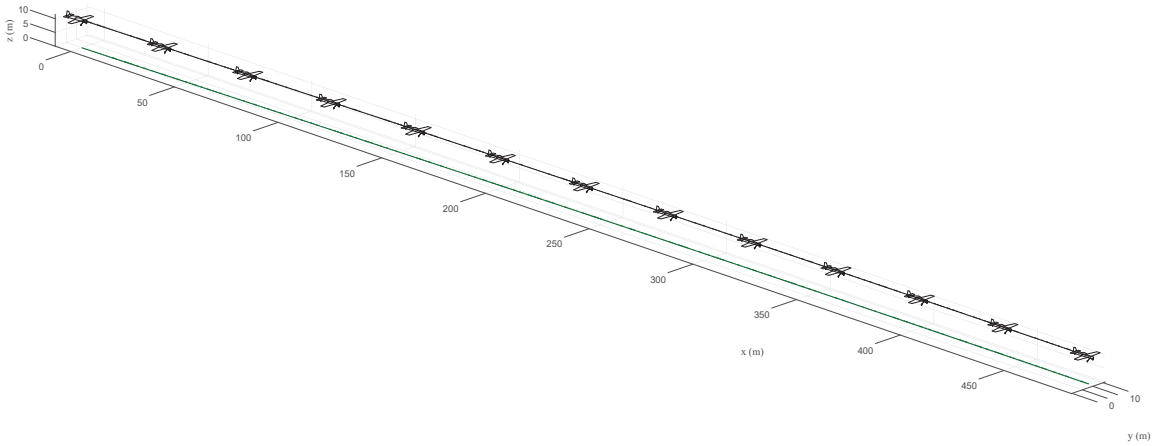

Figure 7: Trajectory plot of the trim analysis maneuver performed by flight automator in X-Plane (the aircraft is drawn once every 1.0 s).

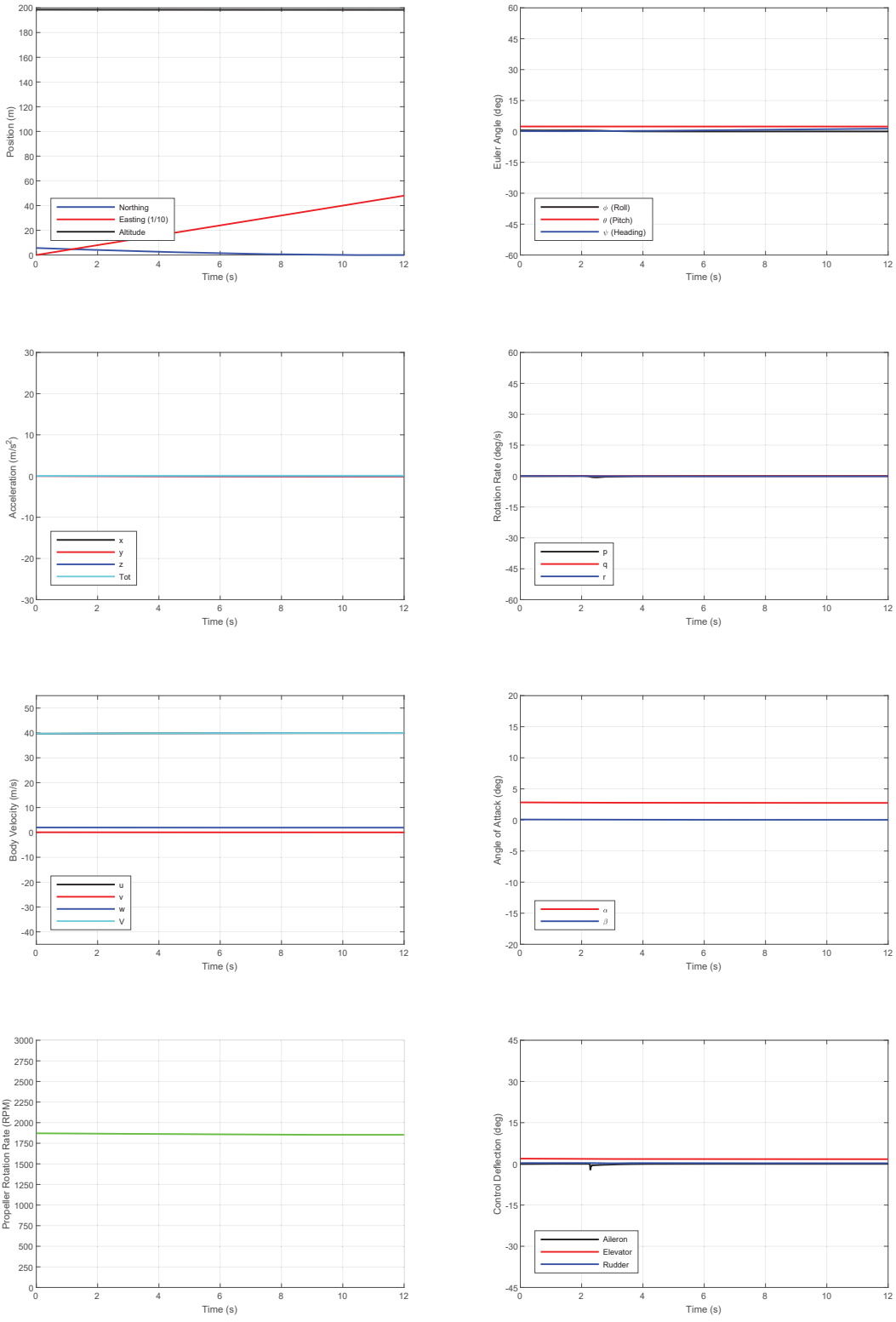

Figure 8: A time history of the trim analysis maneuver performed by flight automator in X-Plane.

B. Stall Speed

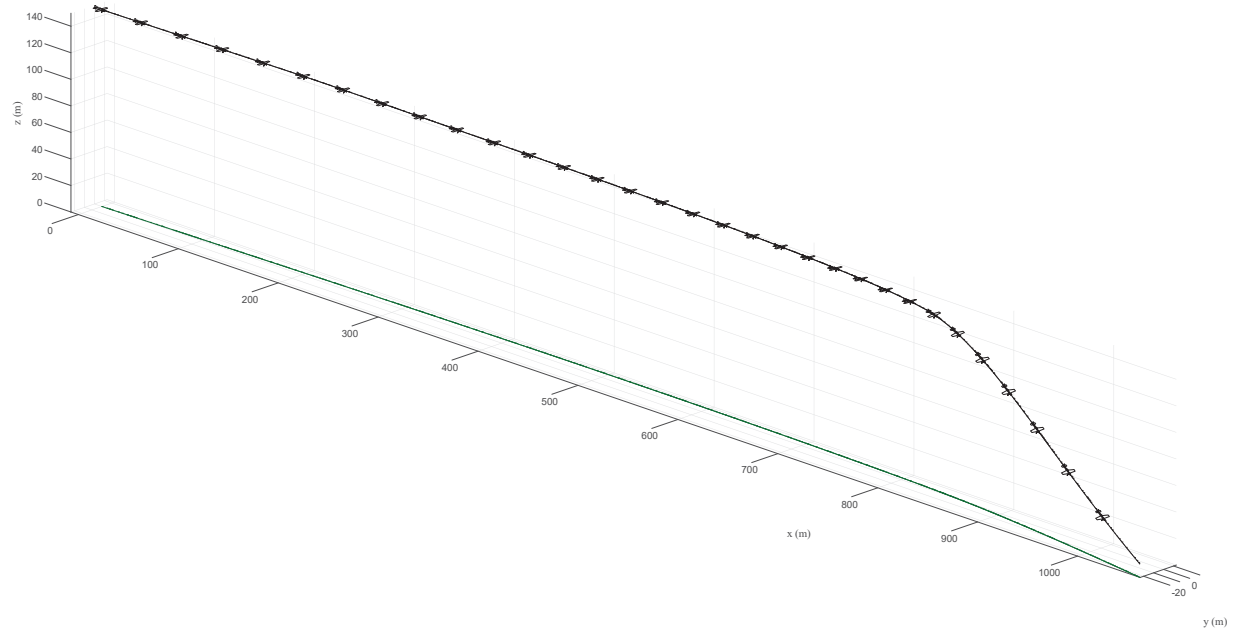

Figure 9: Trajectory plot of the stall speed maneuver performed by flight automator in X-Plane (the aircraft is drawn once every 1.0 s).

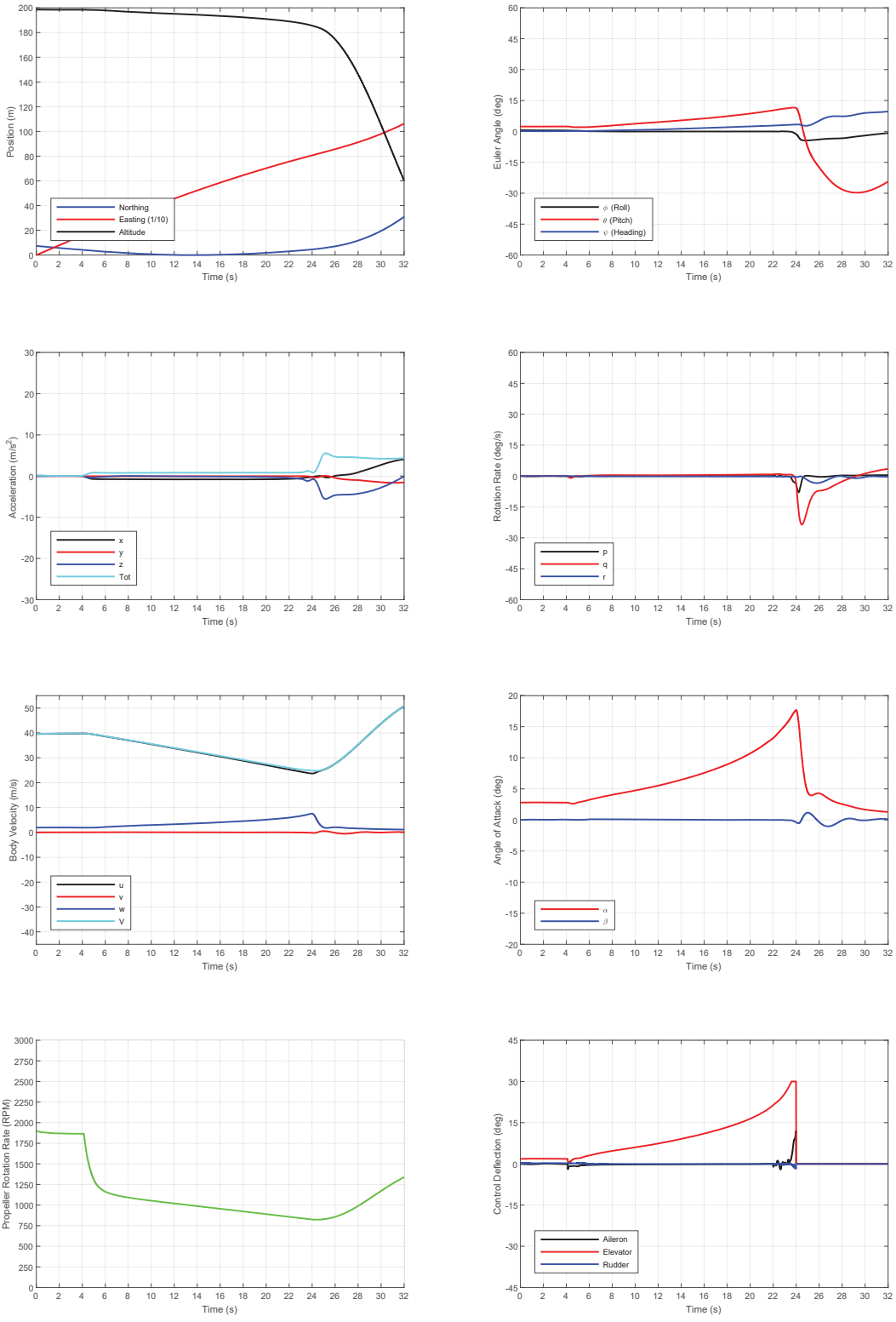

Figure 10: A time history of the stall speed maneuver performed by flight automator in X-Plane.

C. Stall Polar

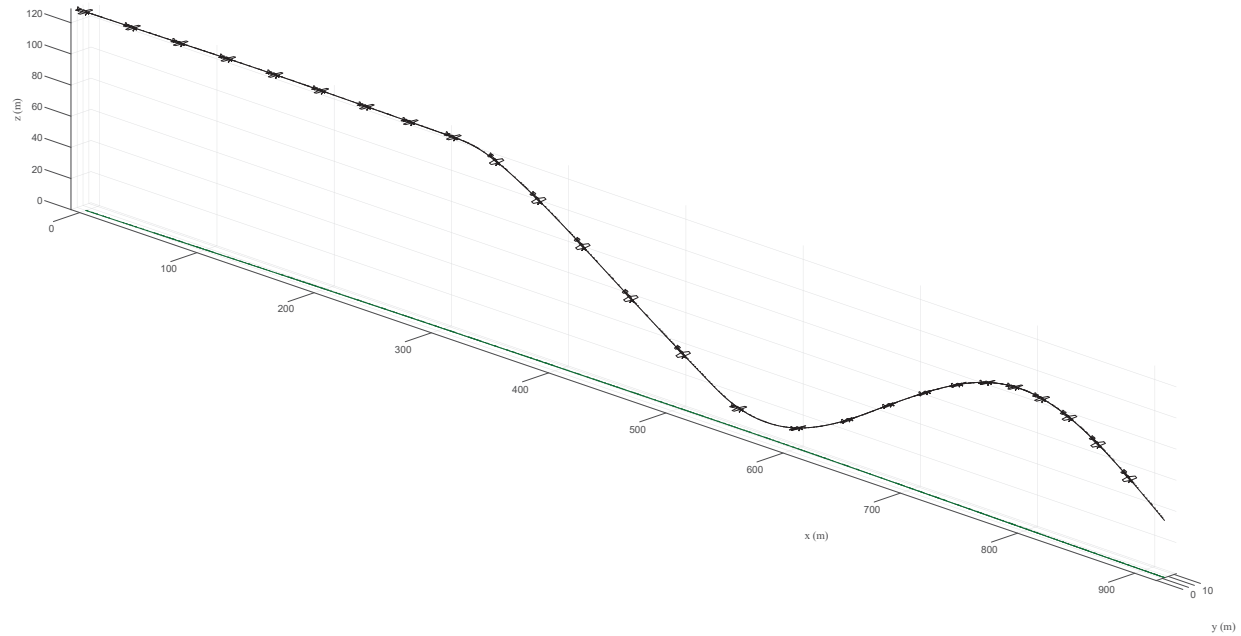

Figure 11: Trajectory plot of the stall polar maneuver performed by flight automator in X-Plane (the aircraft is drawn once every 1.0 s).

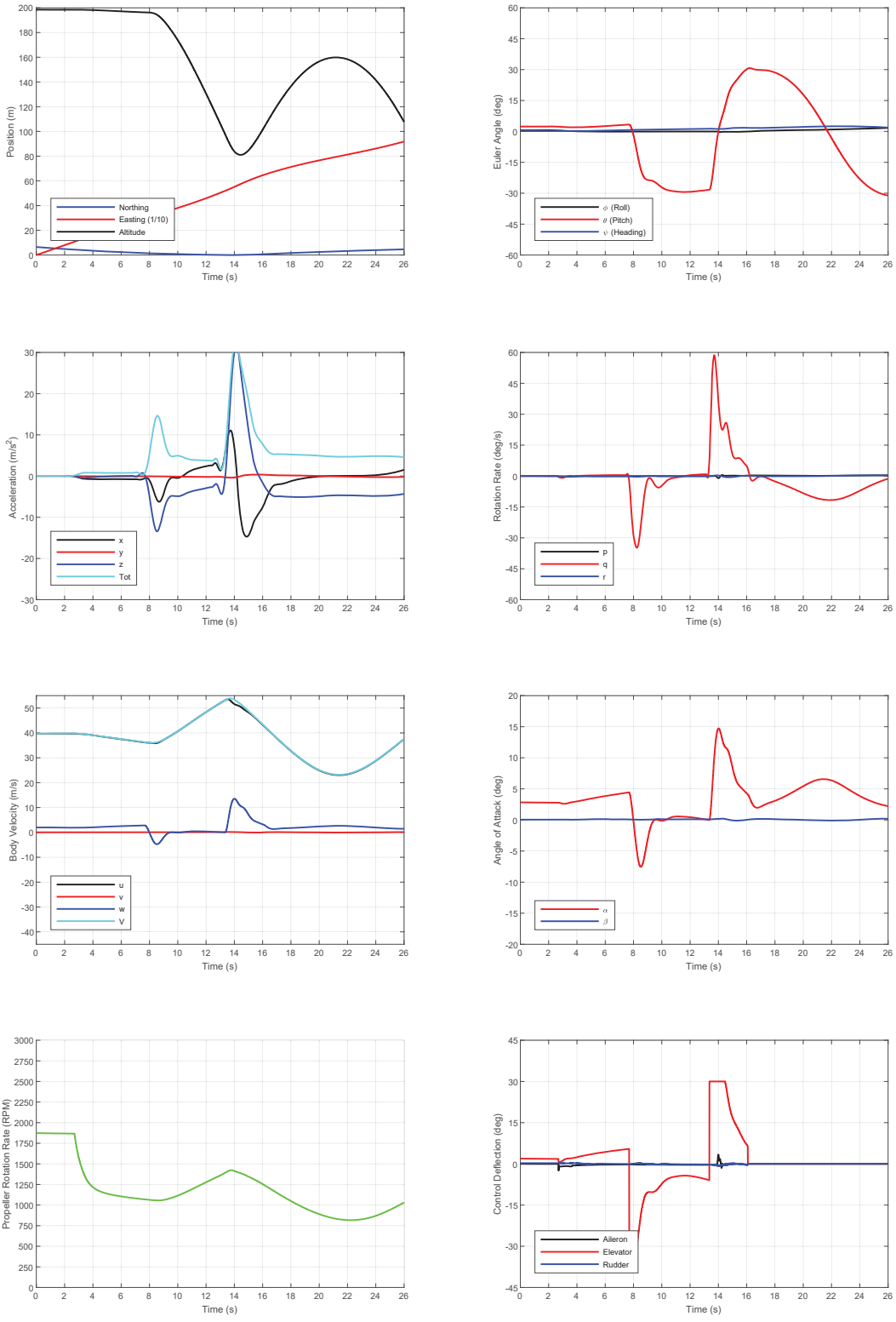

Figure 12: A time history of the stall polar maneuver performed by flight automator in X-Plane.

D. Phugoid

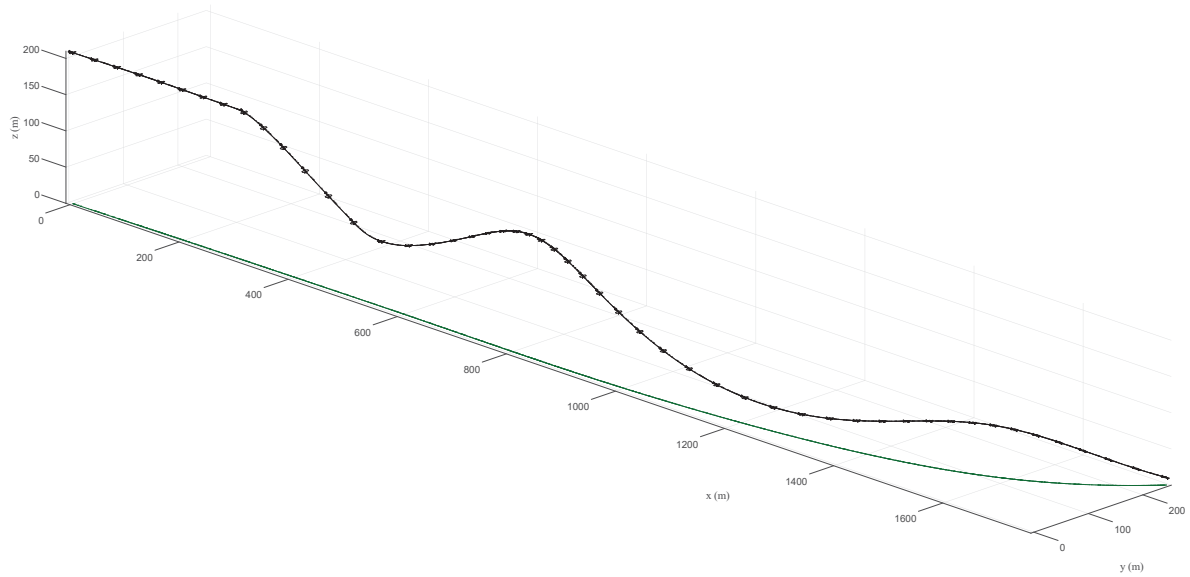

Figure 13: Trajectory plot of the phugoid maneuver performed by flight automator in X-Plane (the aircraft is drawn once every 1.0 s).

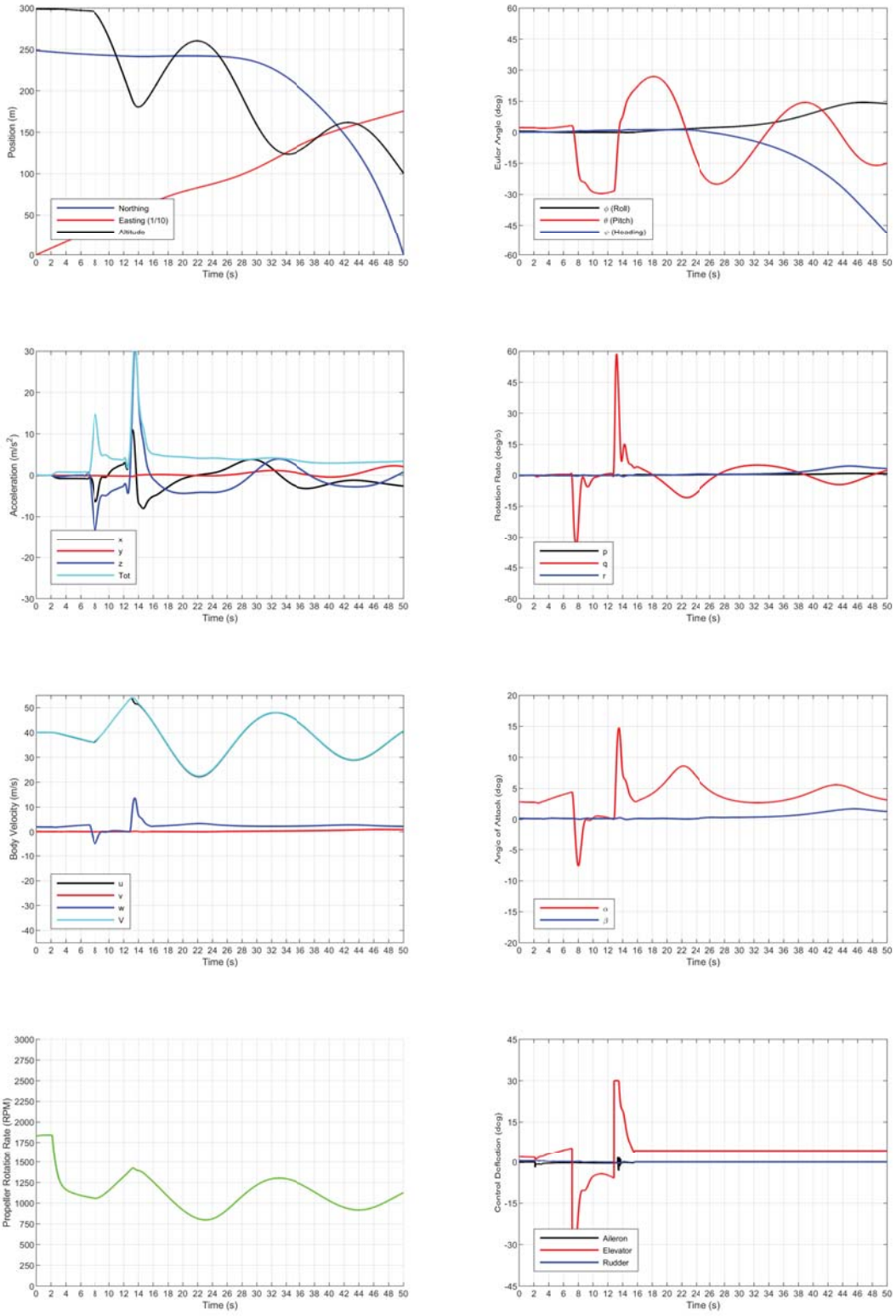

Figure 14: A time history of the phugoid maneuver performed by flight automator in X-Plane.

E. Phugoid with Roll Control

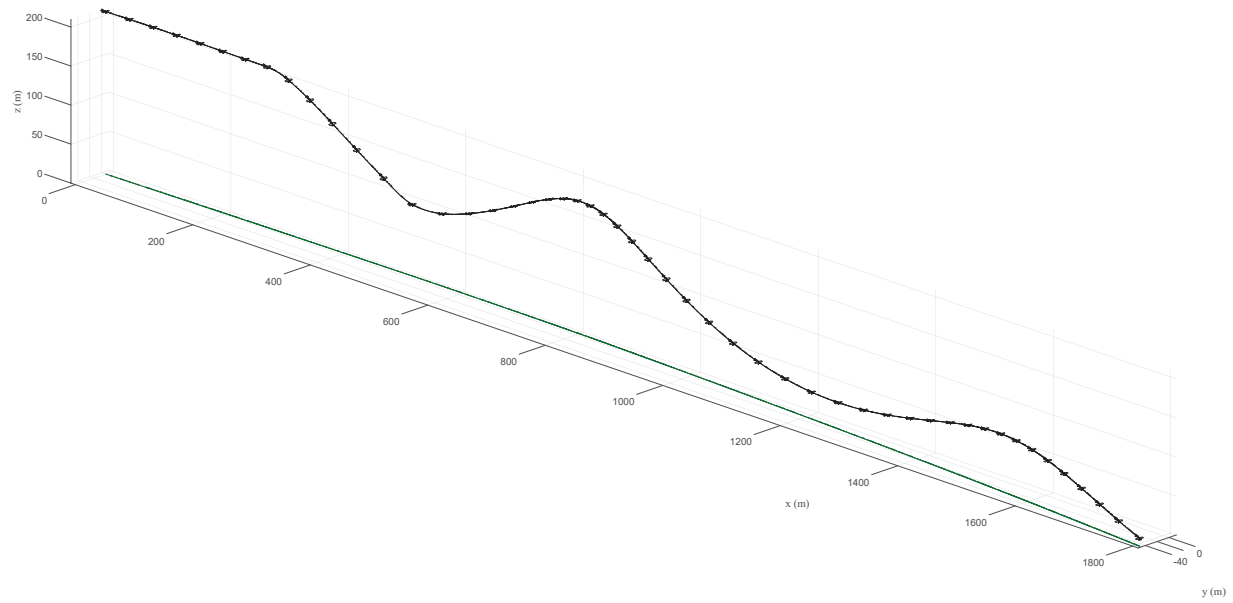

Figure 15: Trajectory plot of the phugoid maneuver with roll control performed by flight automator in X-Plane (the aircraft is drawn once every 1.0 s).

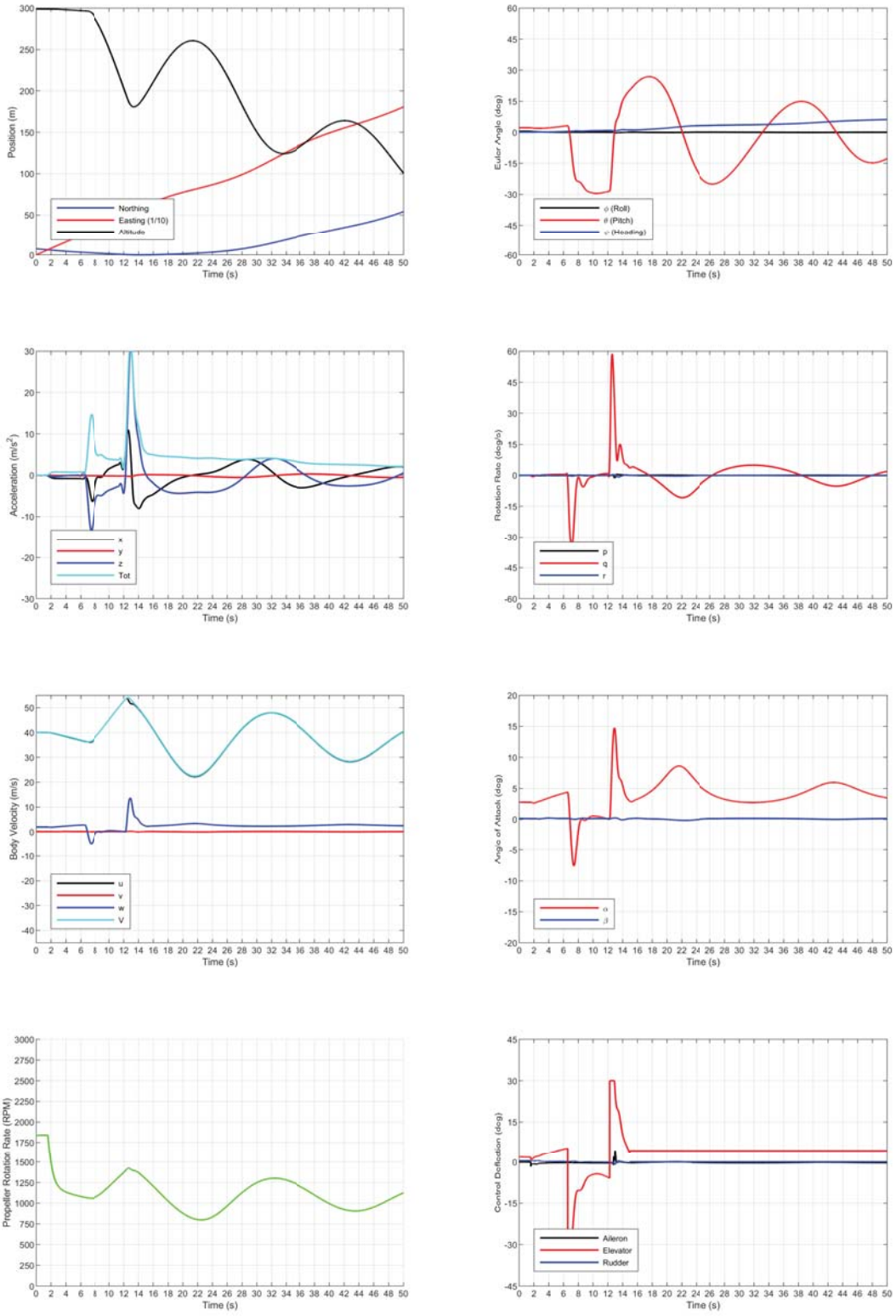

Figure 16: A time history of the phugoid maneuver with roll control performed by flight automator in X-Plane.

F. Idle Descent

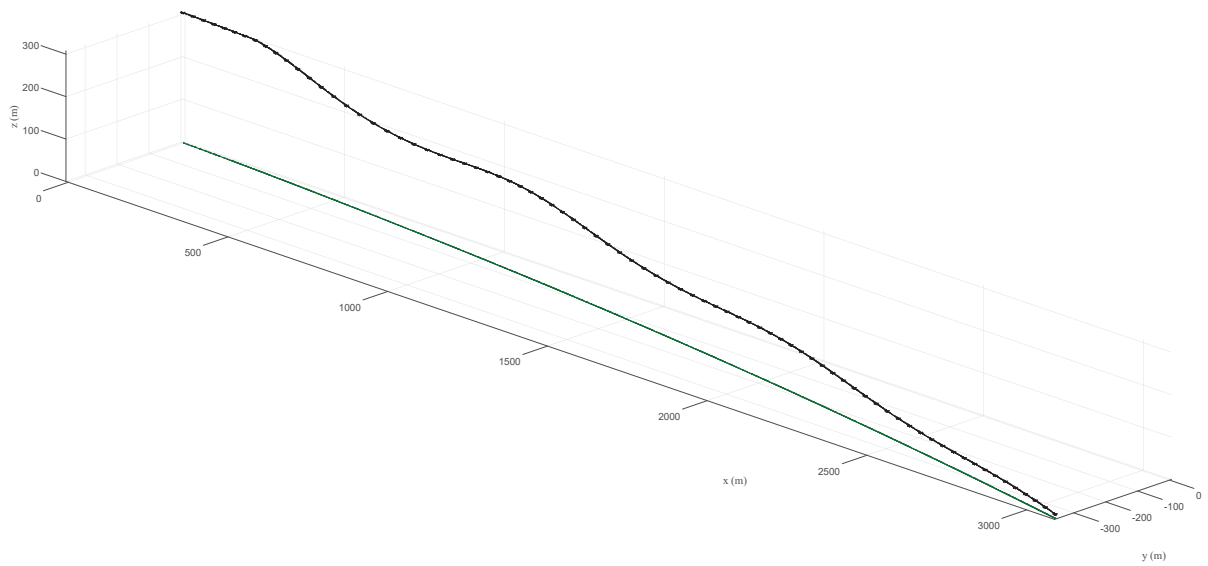

Figure 17: Trajectory plot of the idle descent maneuver performed by flight automator in X-Plane (the aircraft is drawn once every 1.0 s).

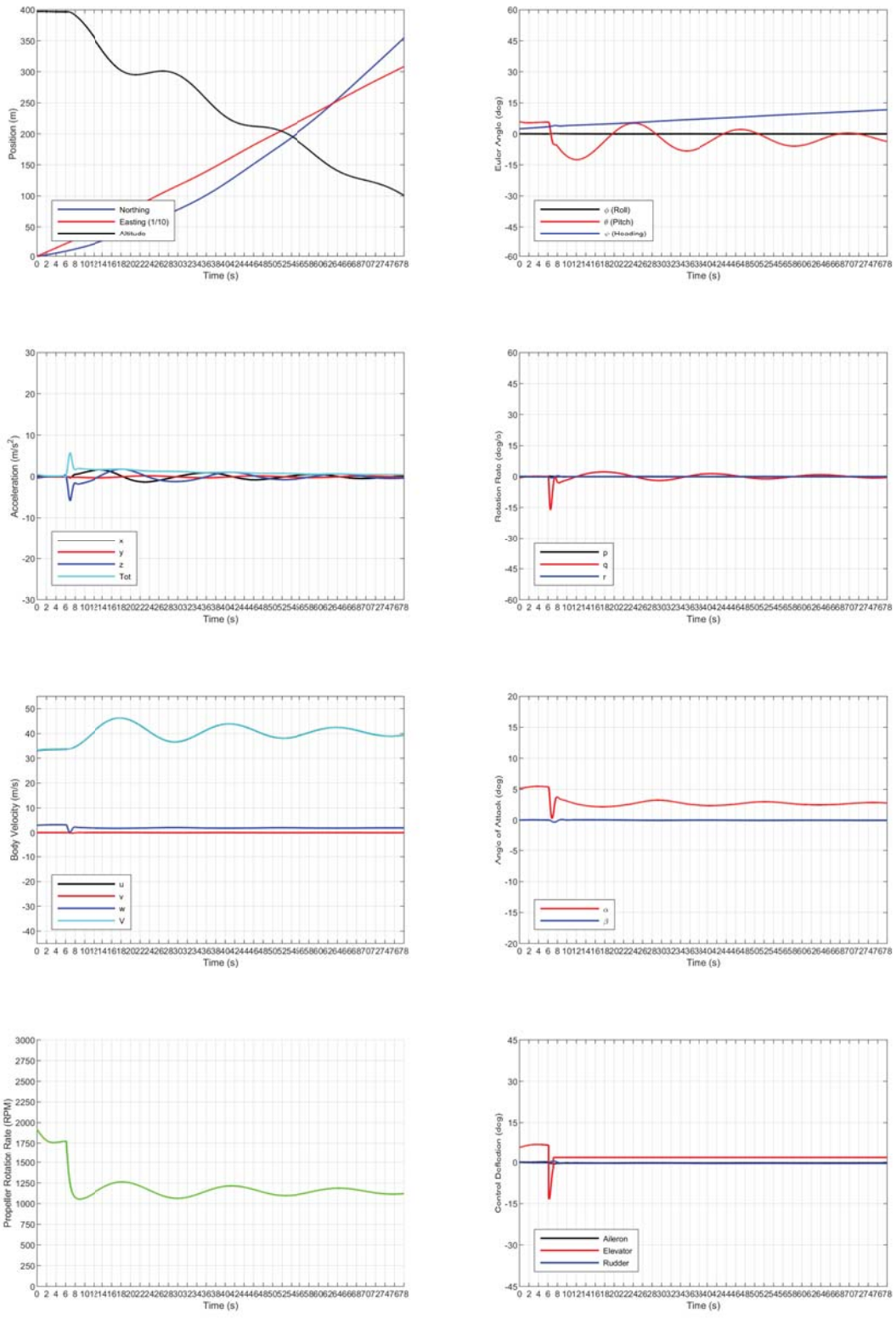

Figure 18: A time history of the idle descent maneuver performed by flight automator in X-Plane.

G. Roll Singlet

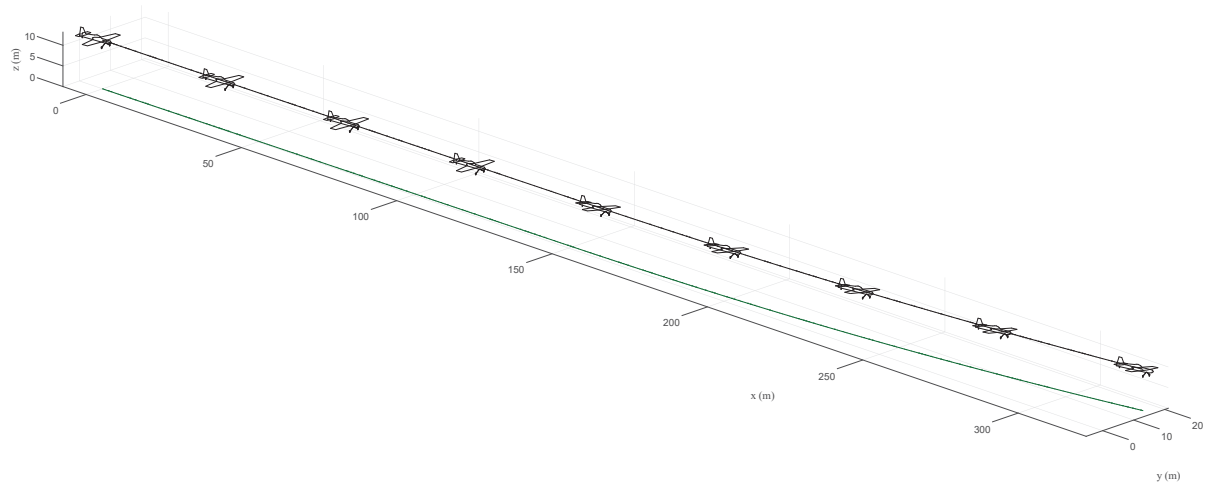

Figure 19: Trajectory plot of the roll singlet maneuver performed by flight automator in X-Plane (the aircraft is drawn once every 1.0 s).

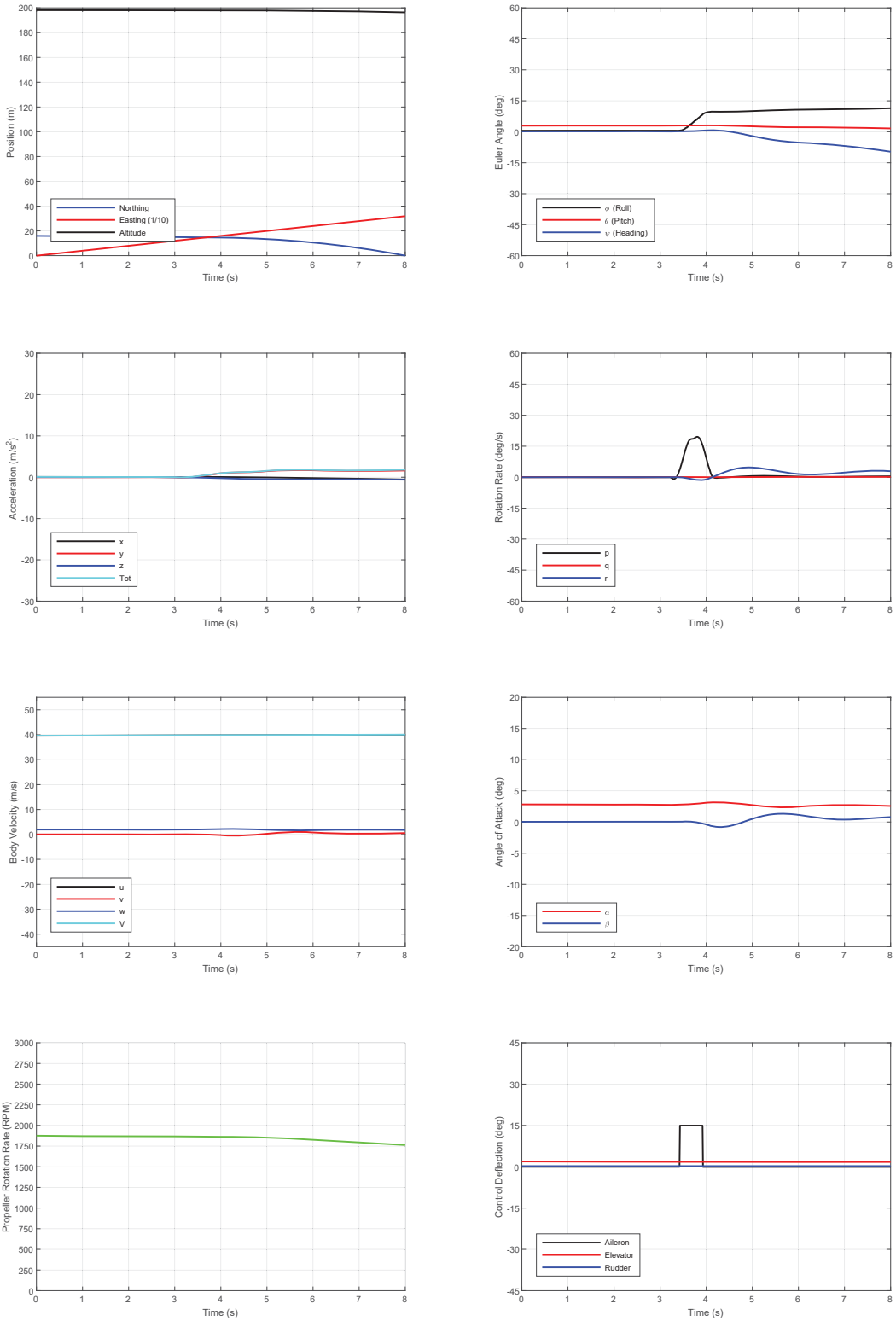

Figure 20: A time history of the roll singlet maneuver performed by flight automator in X-Plane.

H. Roll Doublet

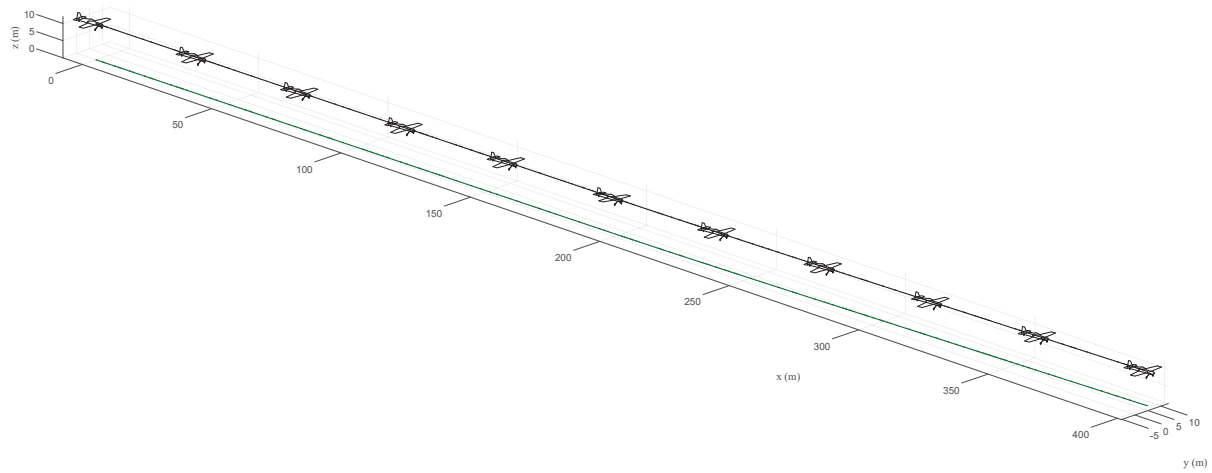

Figure 21: Trajectory plot of the roll doublet maneuver performed by flight automator in X-Plane (the aircraft is drawn once every 1.0 s).

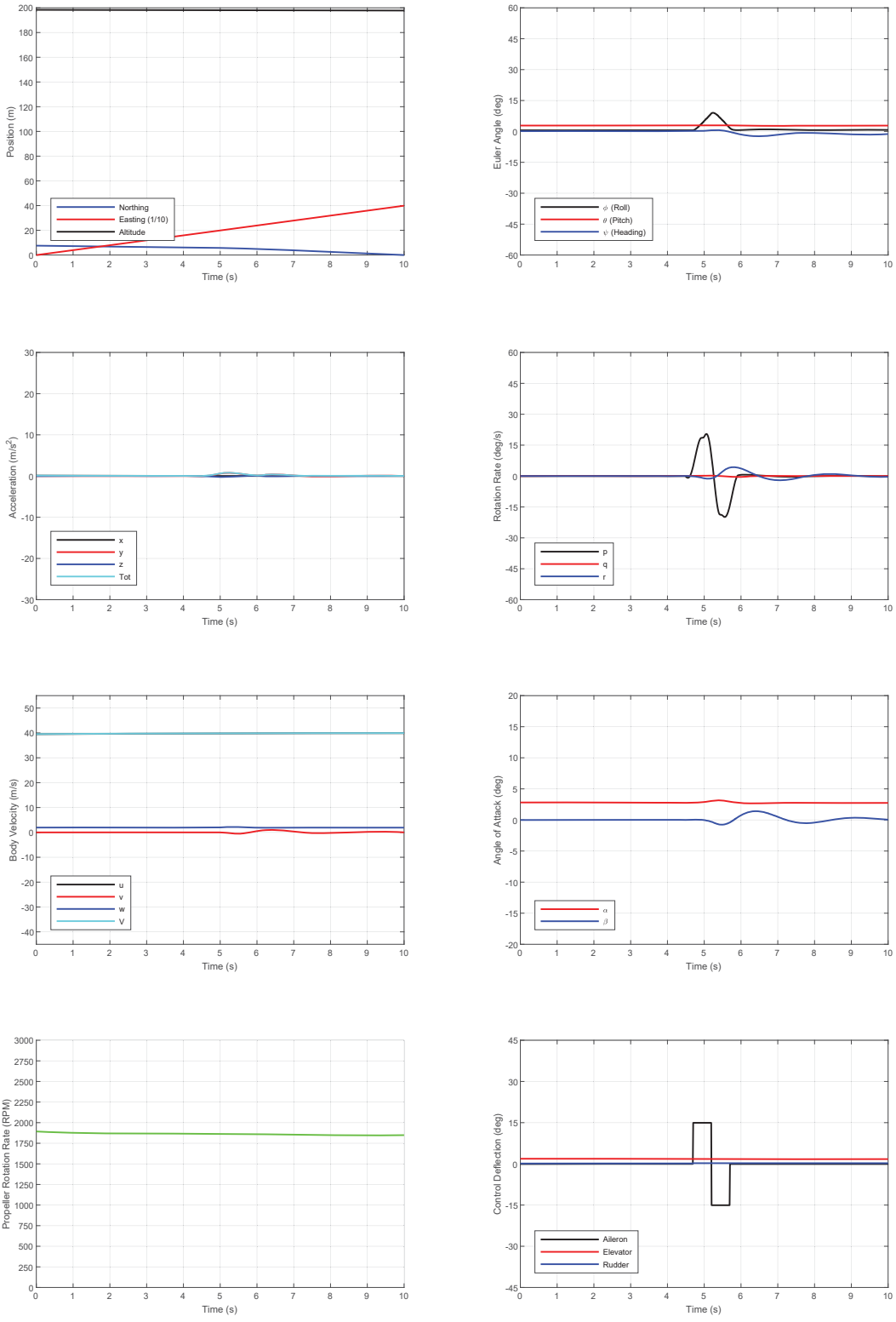

Figure 22: A time history of the roll doublet maneuver performed by flight automator in X-Plane.

I. Pitch Singlet

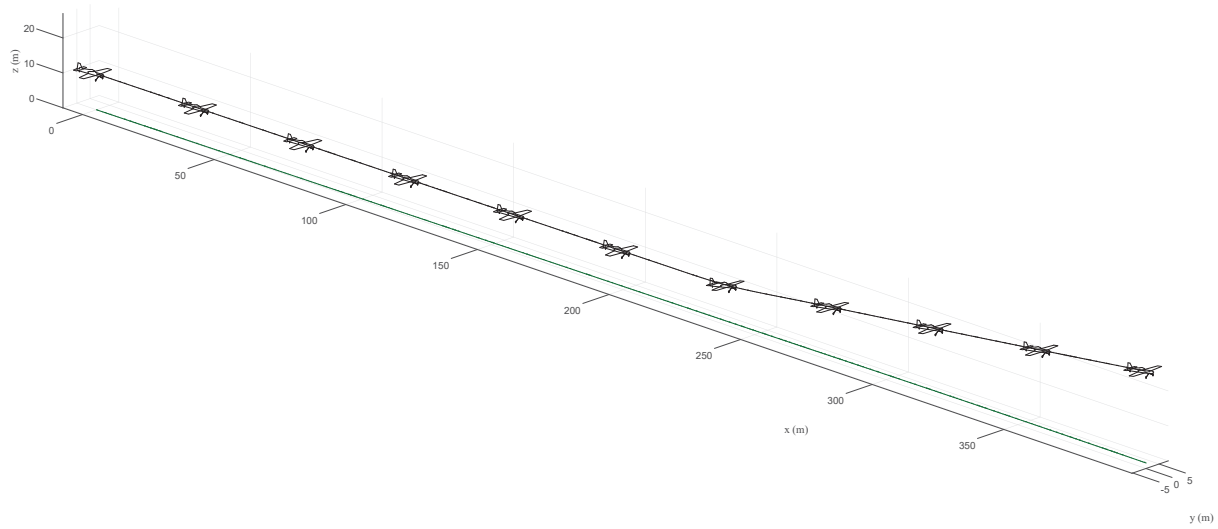

Figure 23: Trajectory plot of the pitch singlet maneuver performed by flight automator in X-Plane (the aircraft is drawn once every 1.0 s).

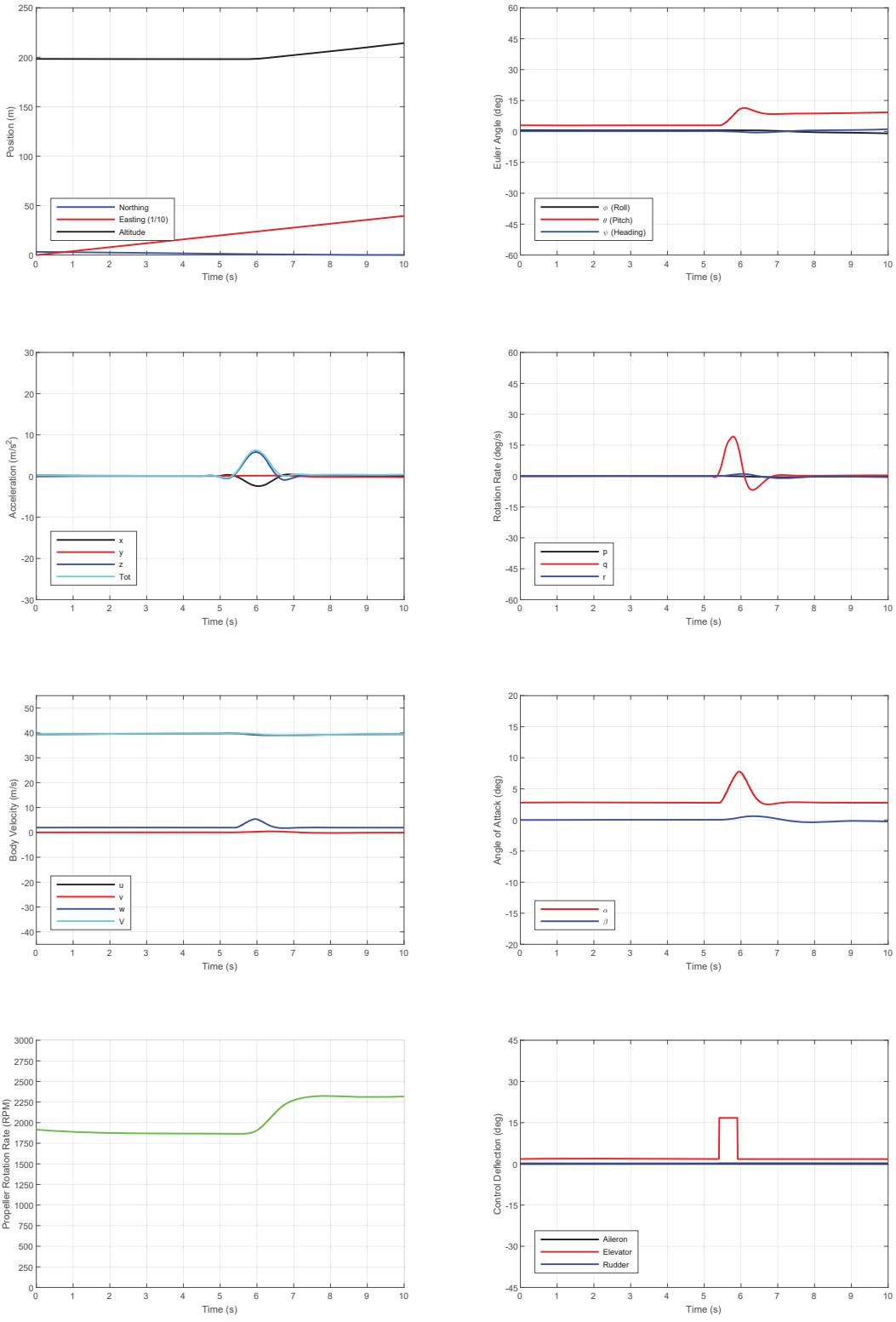

Figure 24: A time history of the pitch singlet maneuver performed by flight automator in X-Plane.

J. Pitch Doublet

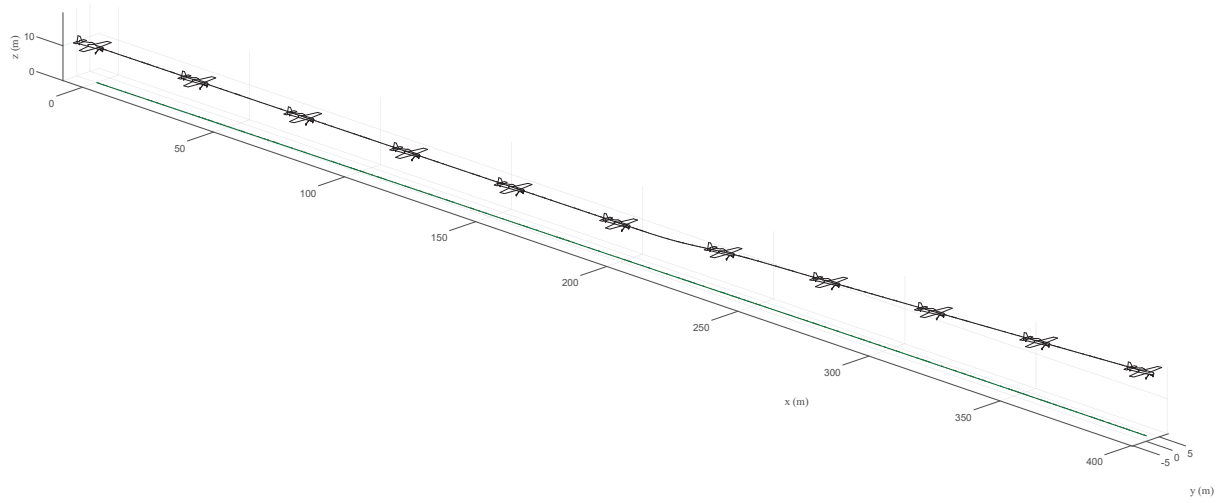

Figure 25: Trajectory plot of the pitch doublet maneuver performed by flight automator in X-Plane (the aircraft is drawn once every 1.0 s).

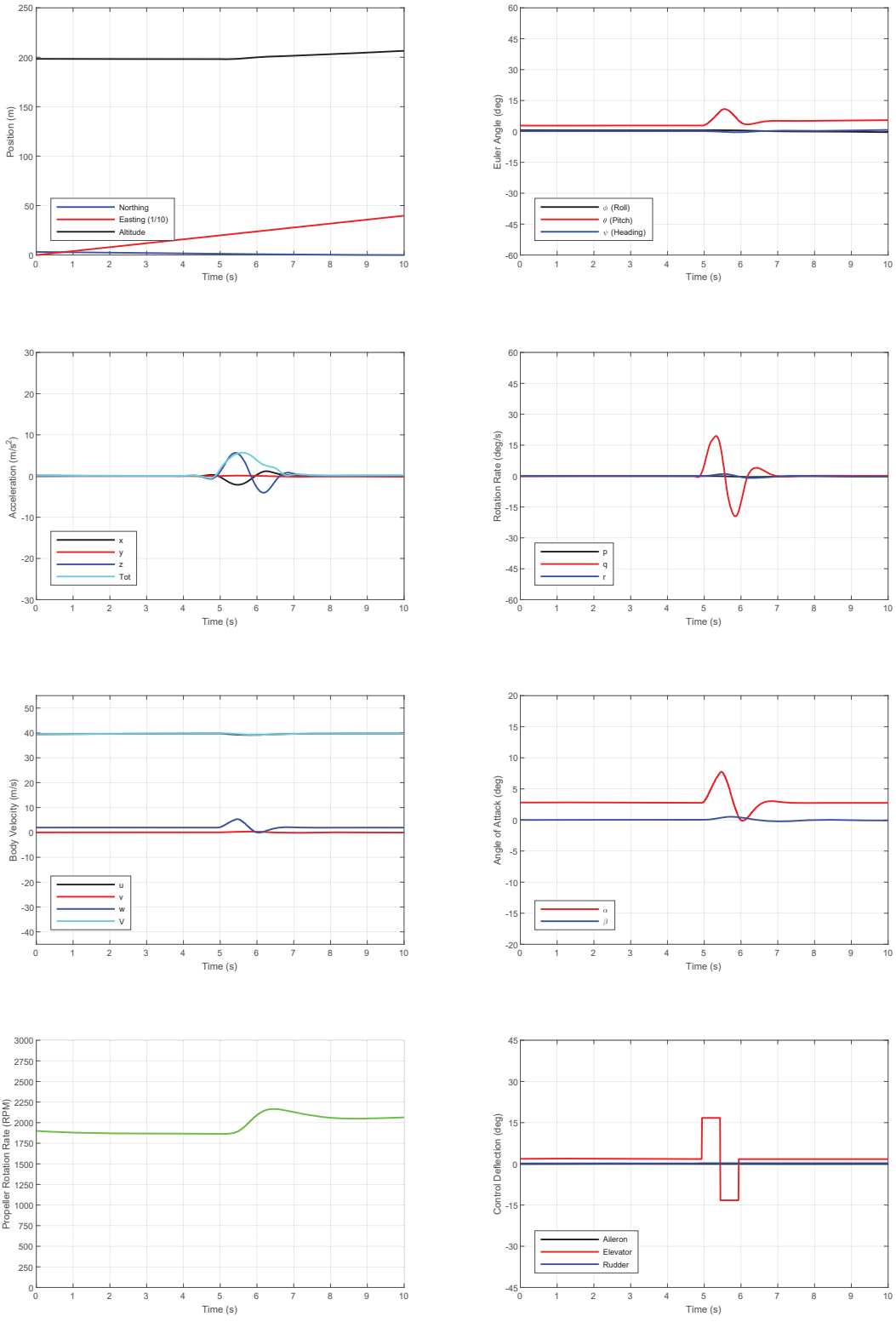

Figure 26: A time history of the pitch doublet maneuver performed by flight automator in X-Plane.

K. Yaw Singlet

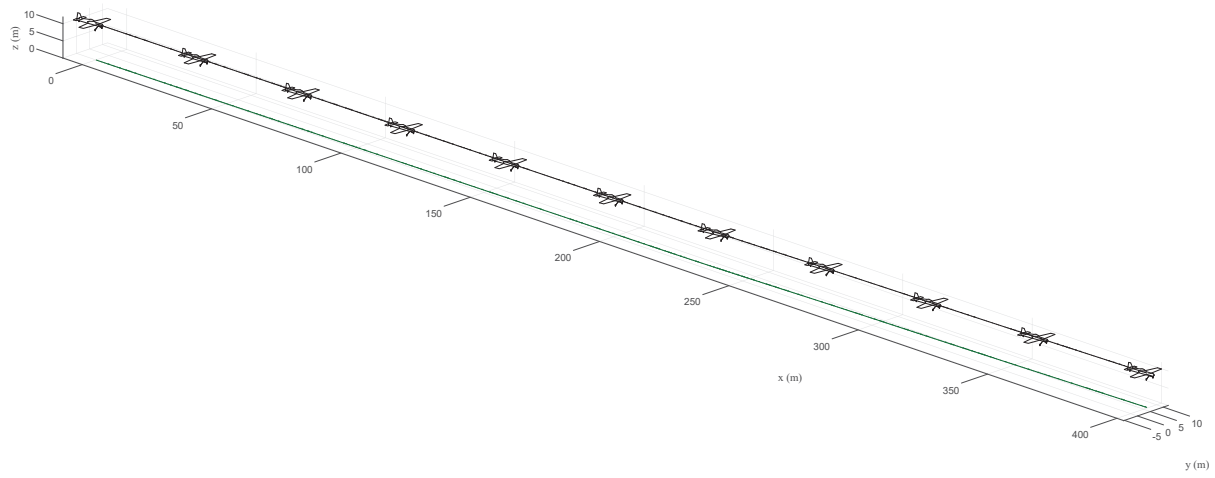

Figure 27: Trajectory plot of the yaw singlet maneuver performed by flight automator in X-Plane (the aircraft is drawn once every 1.0 s).

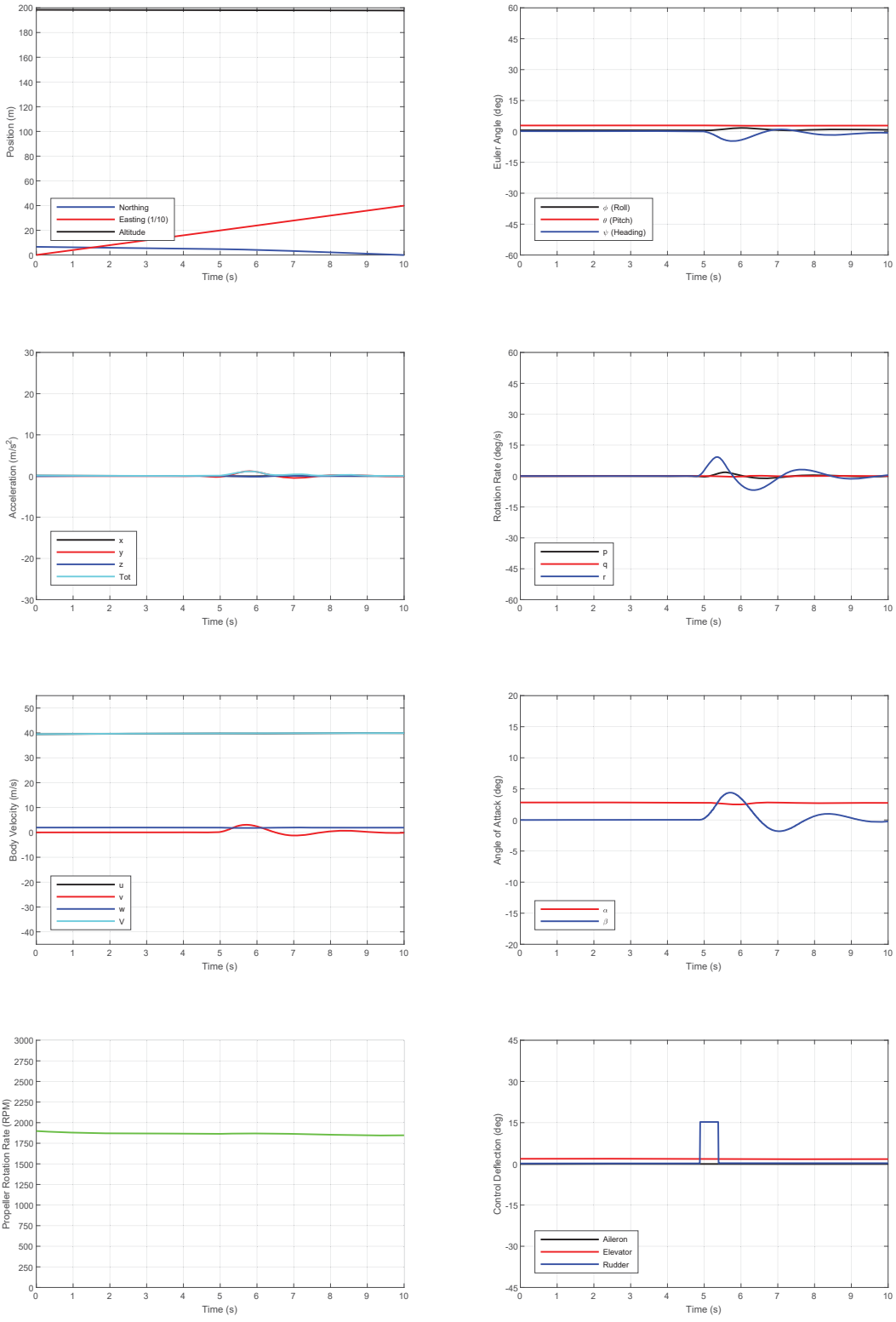

Figure 28: A time history of the yaw singlet maneuver performed by flight automator in X-Plane.

L. Yaw Doublet

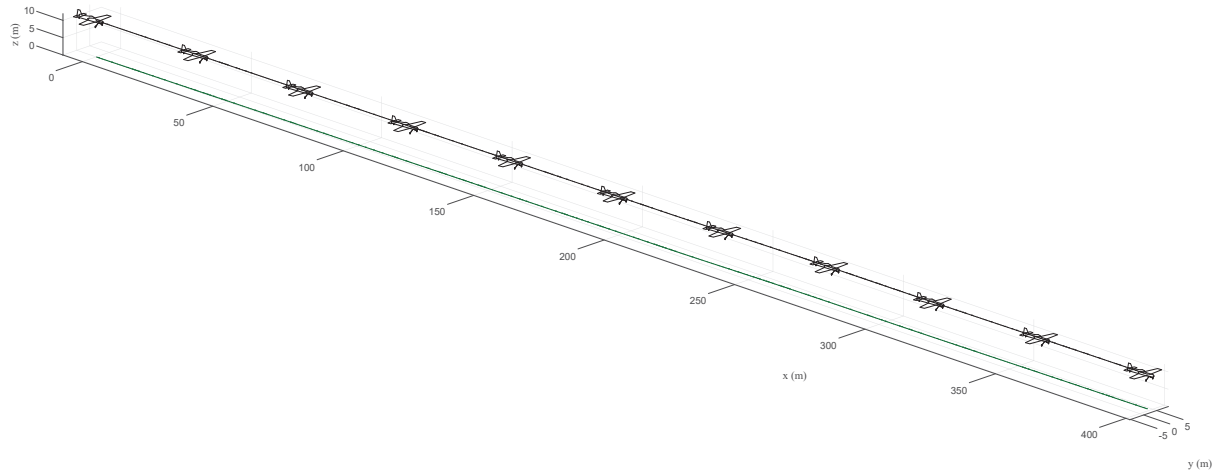

Figure 29: Trajectory plot of the yaw doublet maneuver performed by flight automator in X-Plane (the aircraft is drawn once every 1.0 s).

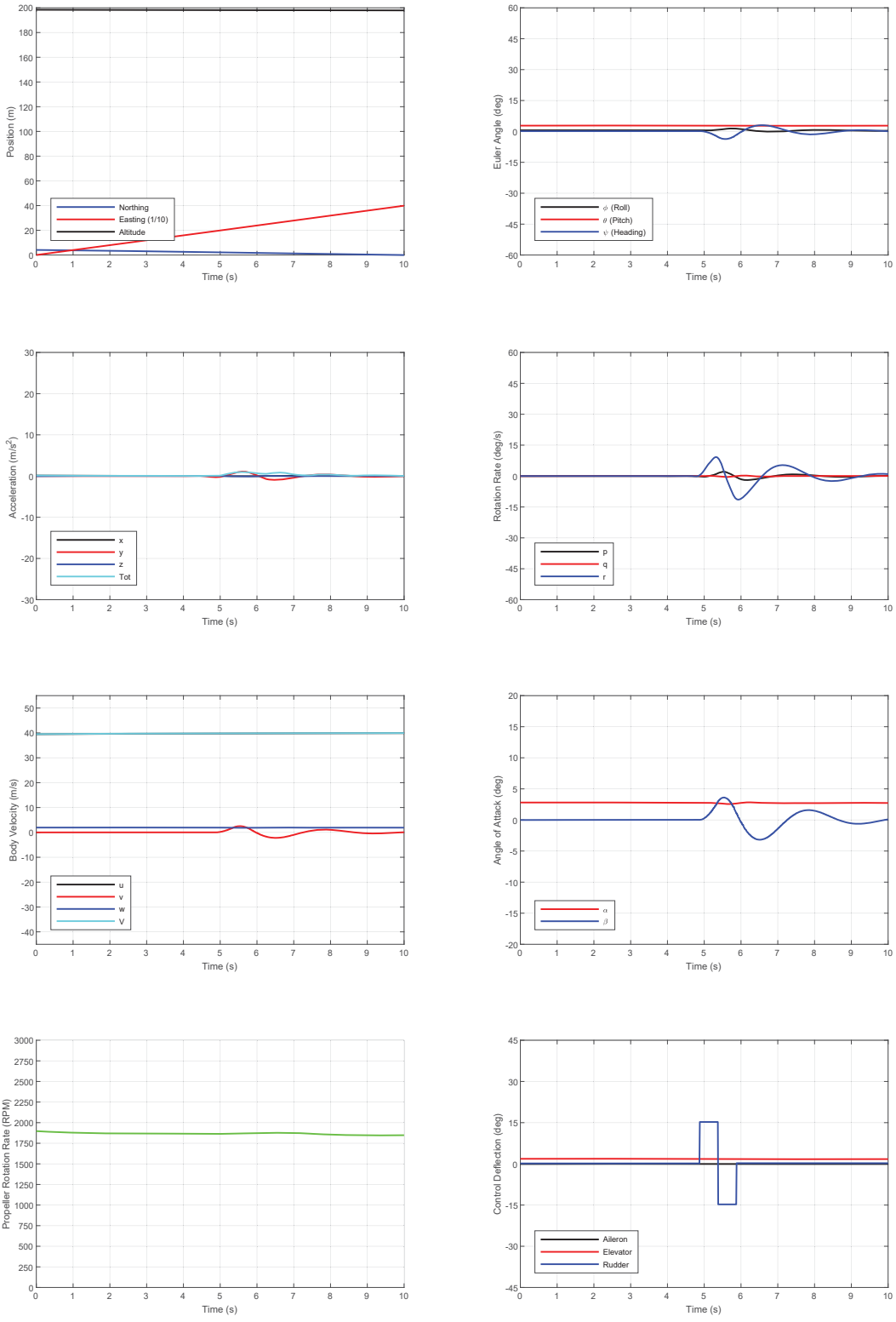

Figure 30: A time history of the yaw doublet maneuver performed by flight automator in X-Plane.

Appendix B: Flight Testing Results

A. Stall Speed

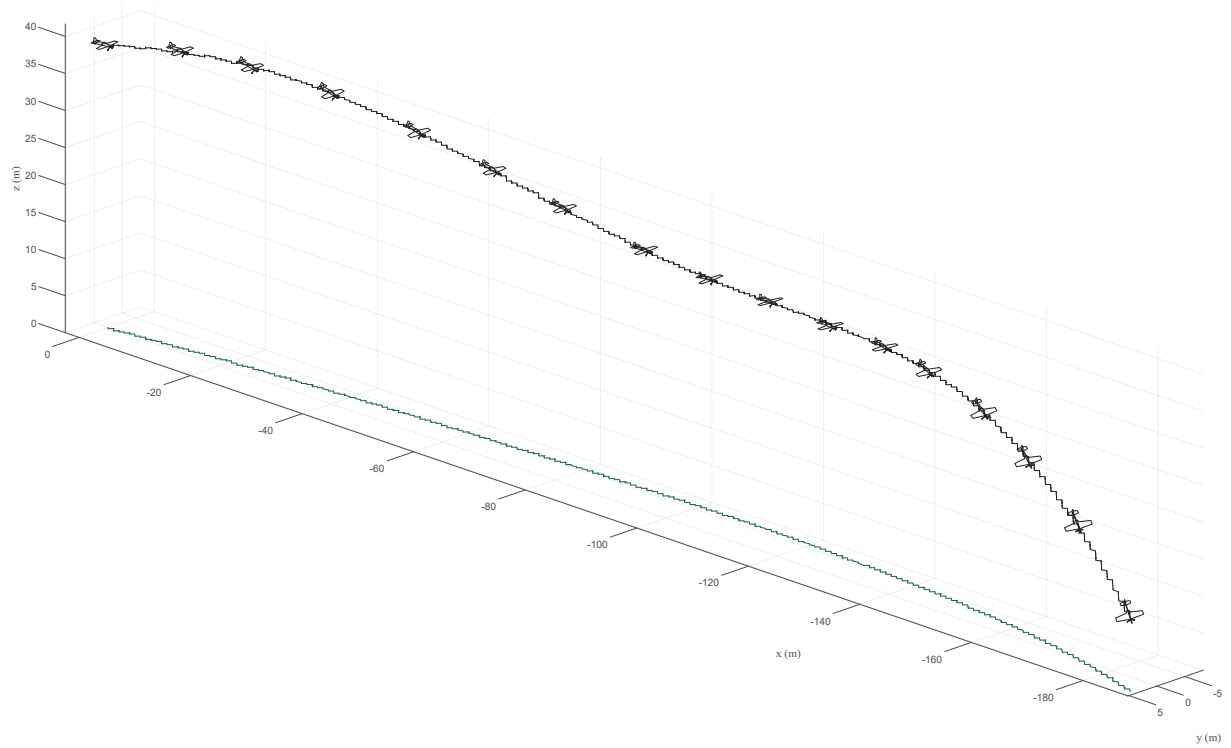

Figure 31: Trajectory plot of the Avistar UAV performing a stall speed maneuver using the flight automator (the aircraft is drawn once every 0.2 s).

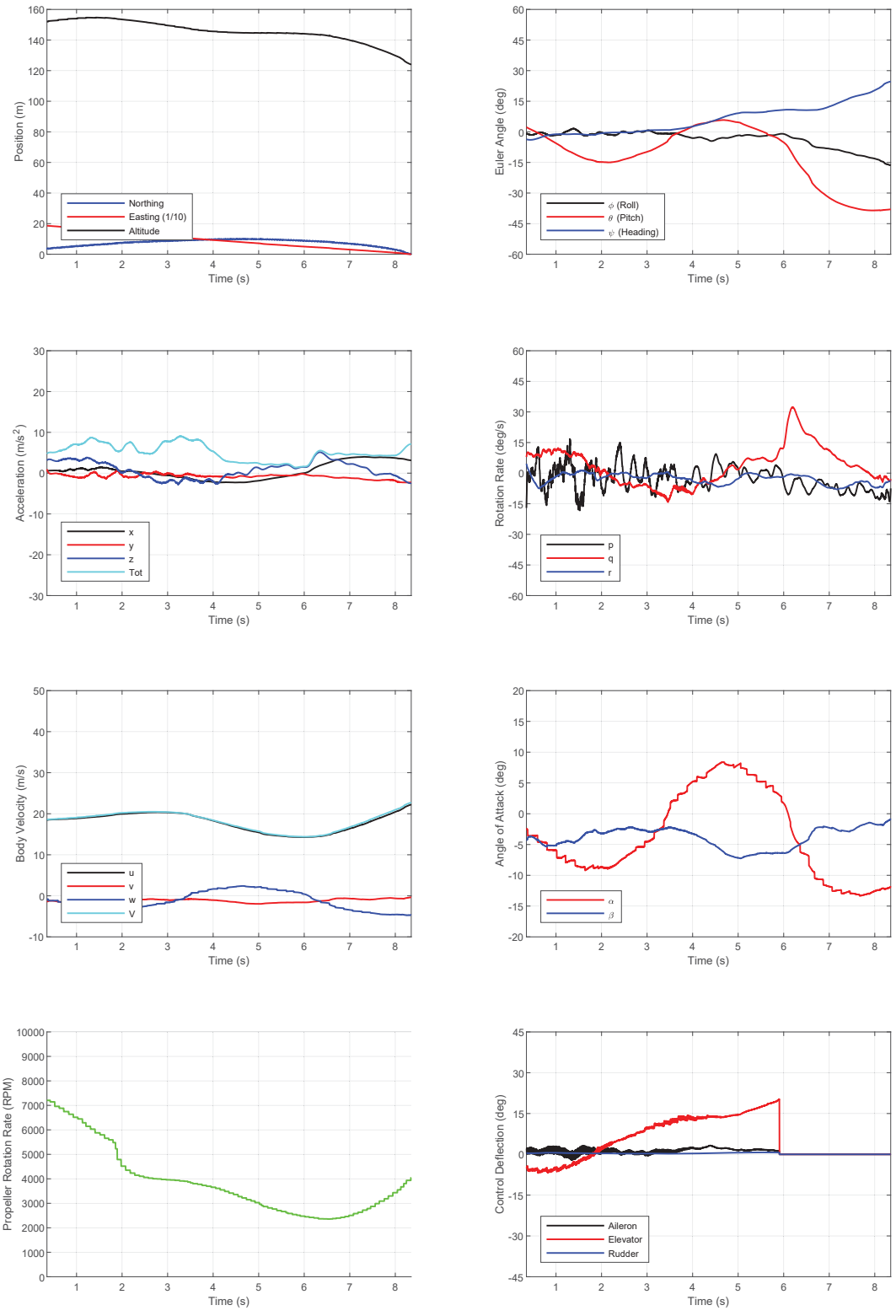

Figure 32: A time history of the Avistar UAV performing a stall speed maneuver using the flight automator.

B. Stall Polar

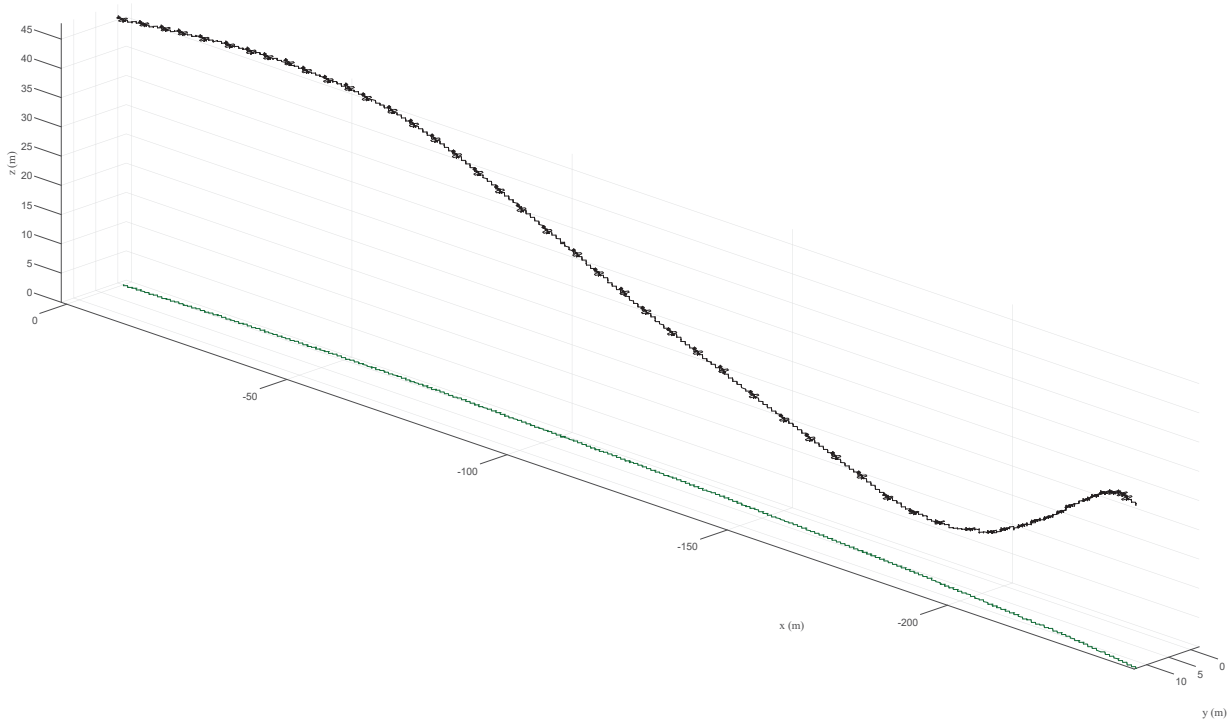

Figure 33: Trajectory plot of the Avistar UAV performing a stall polar maneuver using the flight automator (the aircraft is drawn once every 0.2 s).

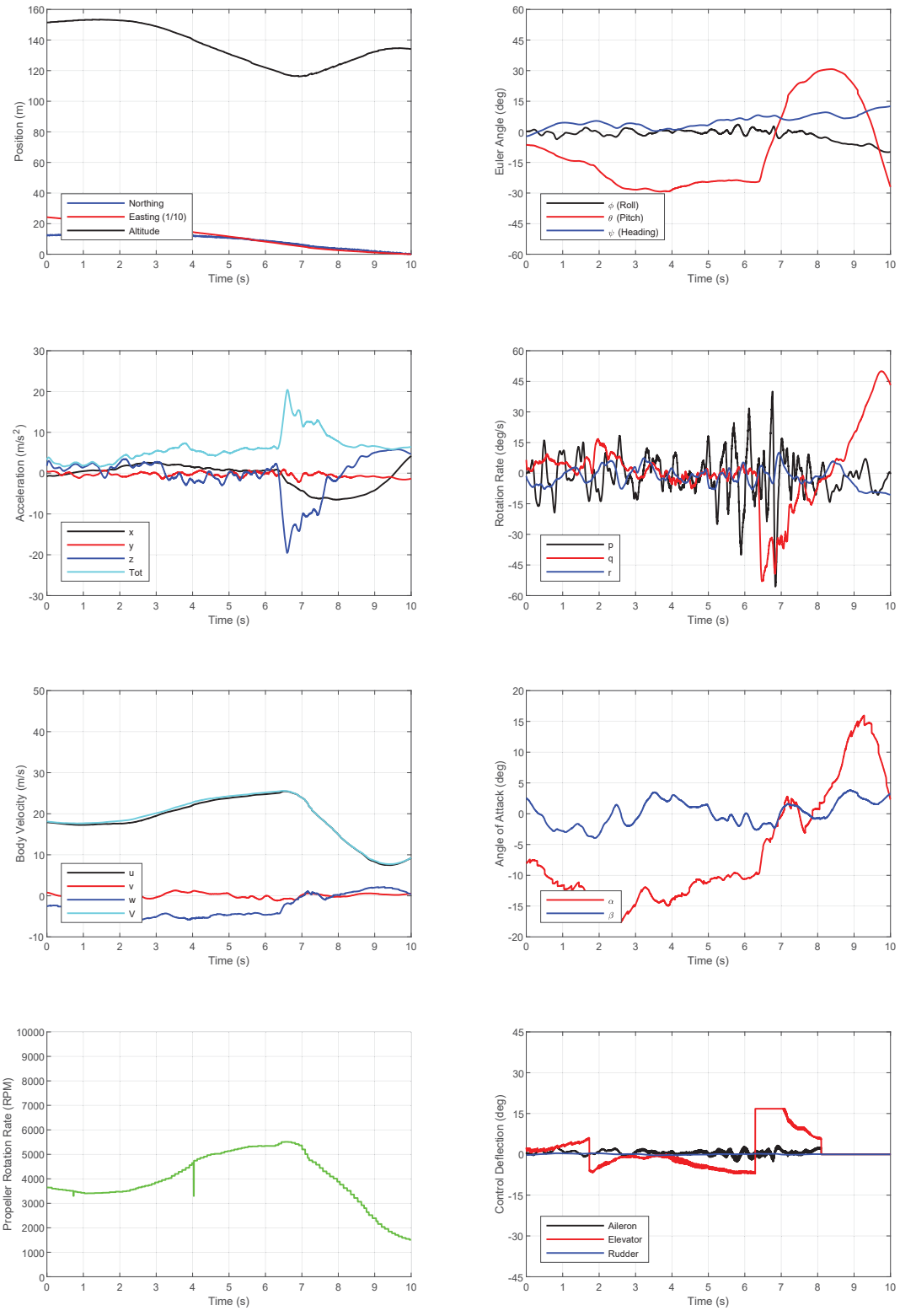

Figure 34: A time history of the Avistar UAV performing a stall polar maneuver using the flight automator.

C. Idle Descent

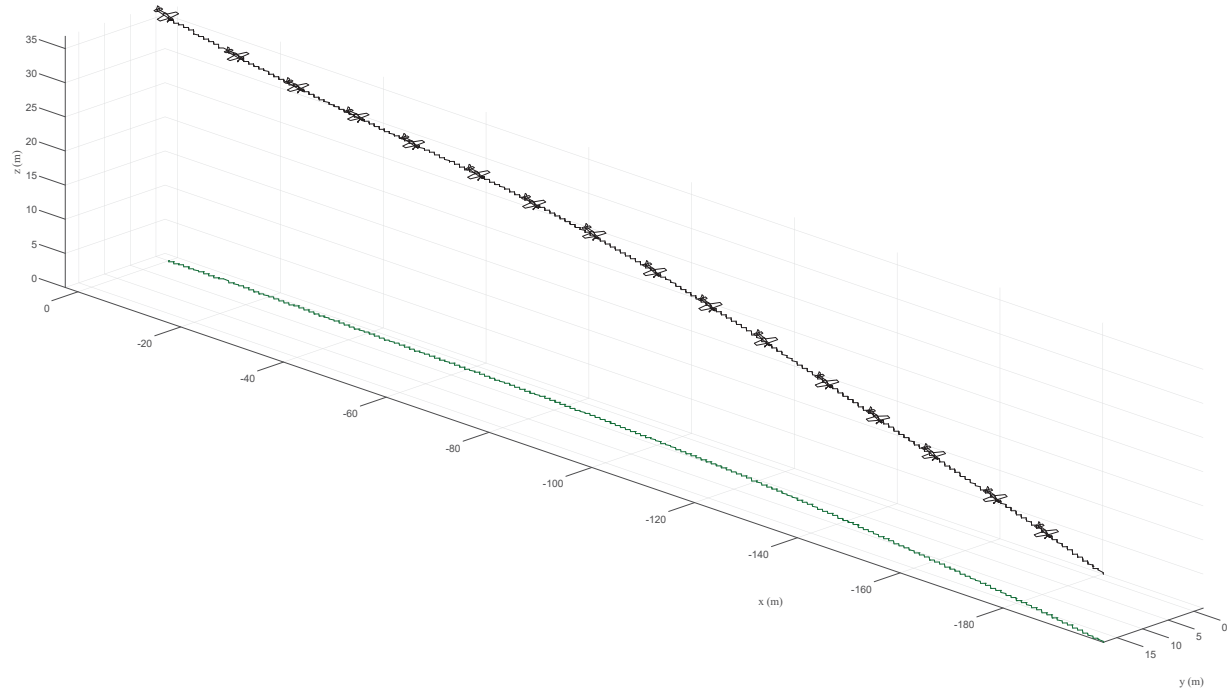

Figure 35: Trajectory plot of the Avistar UAV performing an idle descent maneuver using the flight automator (the aircraft is drawn once every 0.2 s).

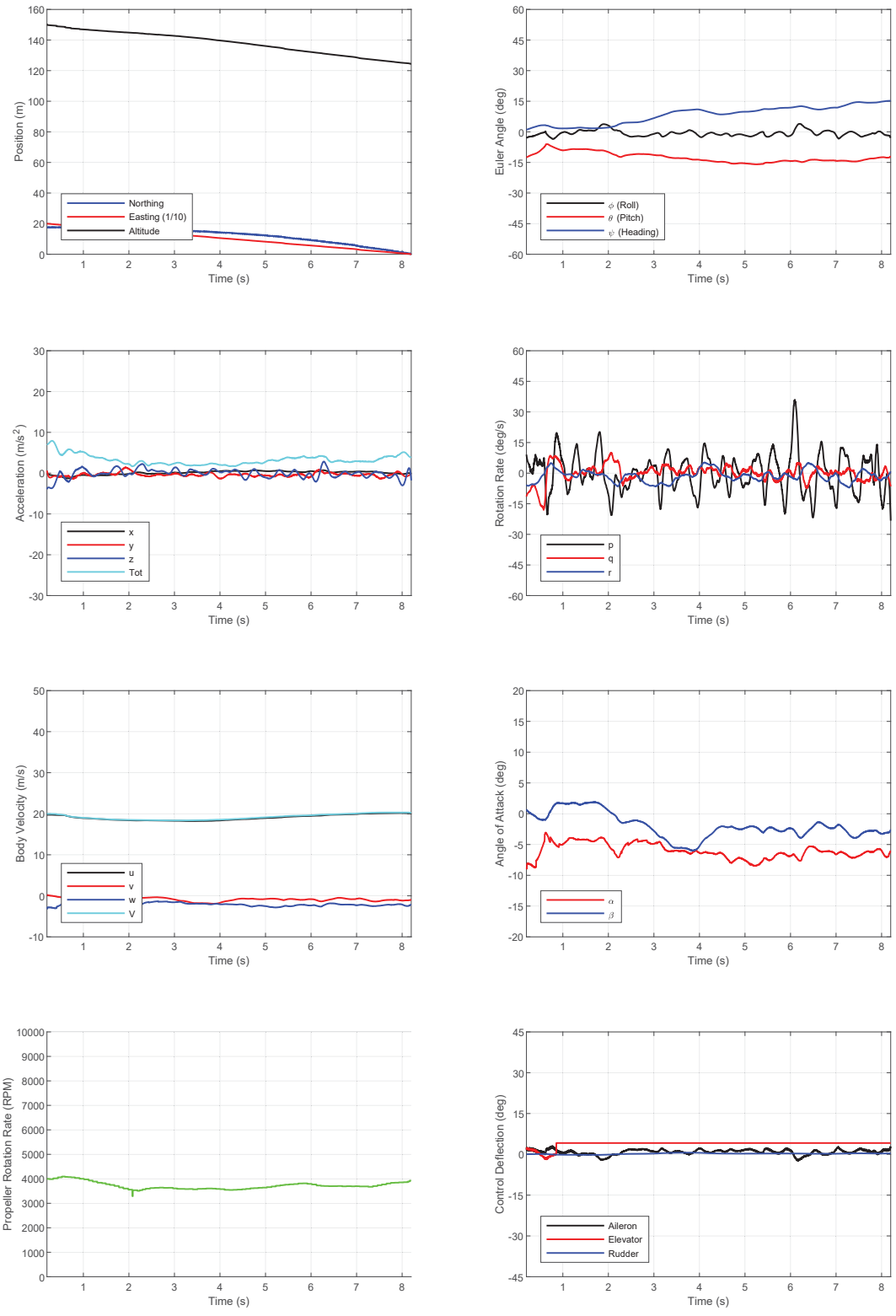

Figure 36: A time history of the Avistar UAV performing an idle descent maneuver using the flight automator.

D. Roll Doublet

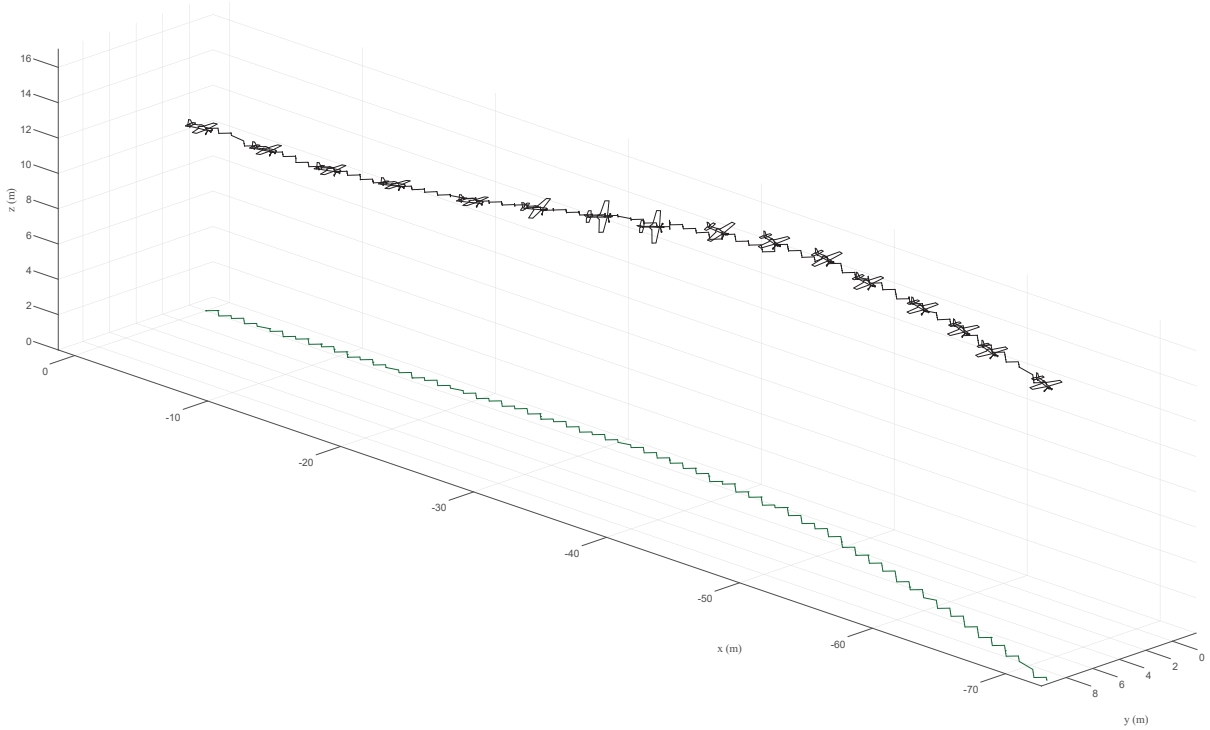

Figure 37: Trajectory plot of the Avistar UAV performing a roll doublet maneuver using the flight automator (the aircraft is drawn once every 0.2 s).

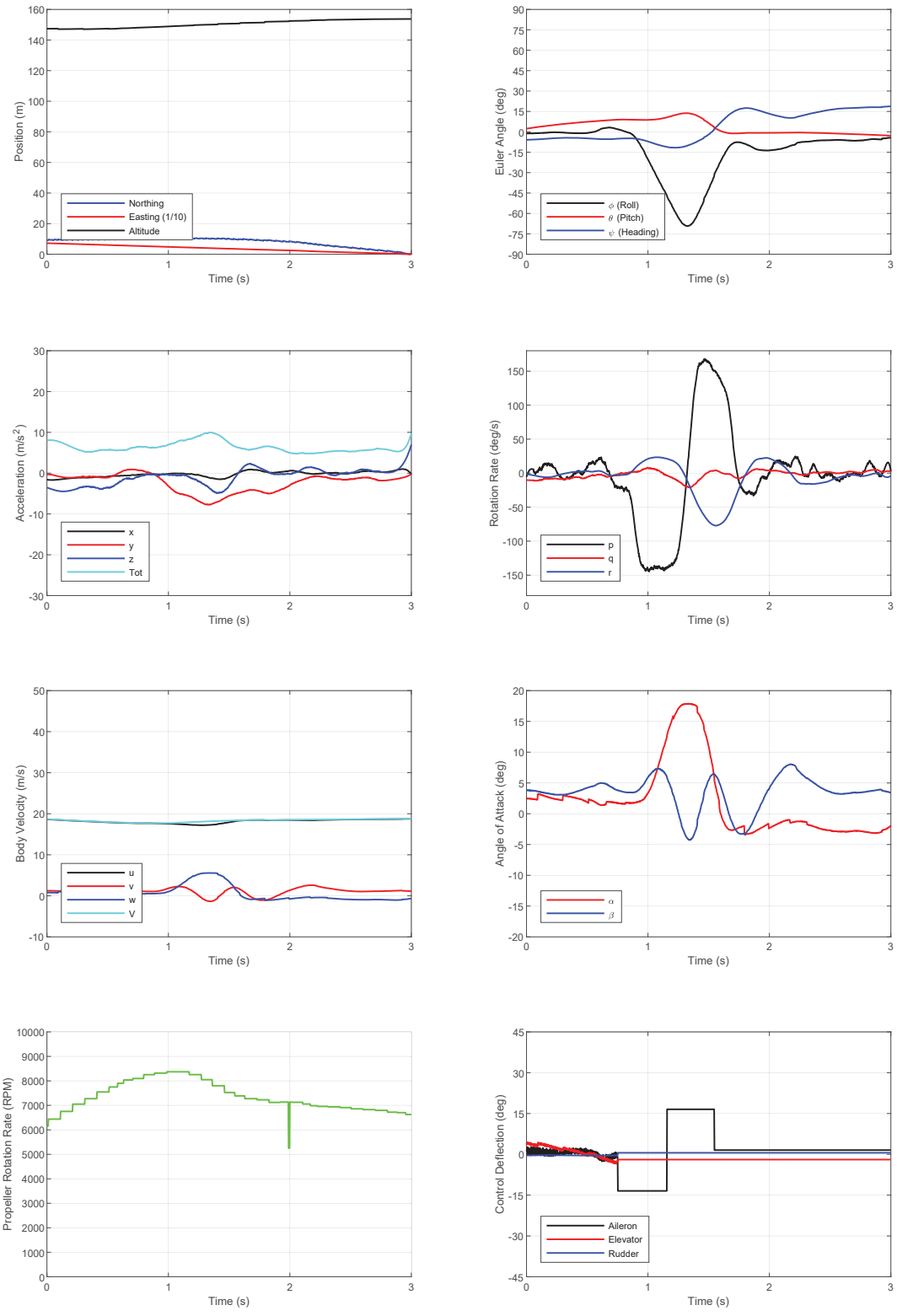

Figure 38: A time history of the Avistar UAV performing a roll doublet maneuver using the flight automator.

E. Pitch Doublet

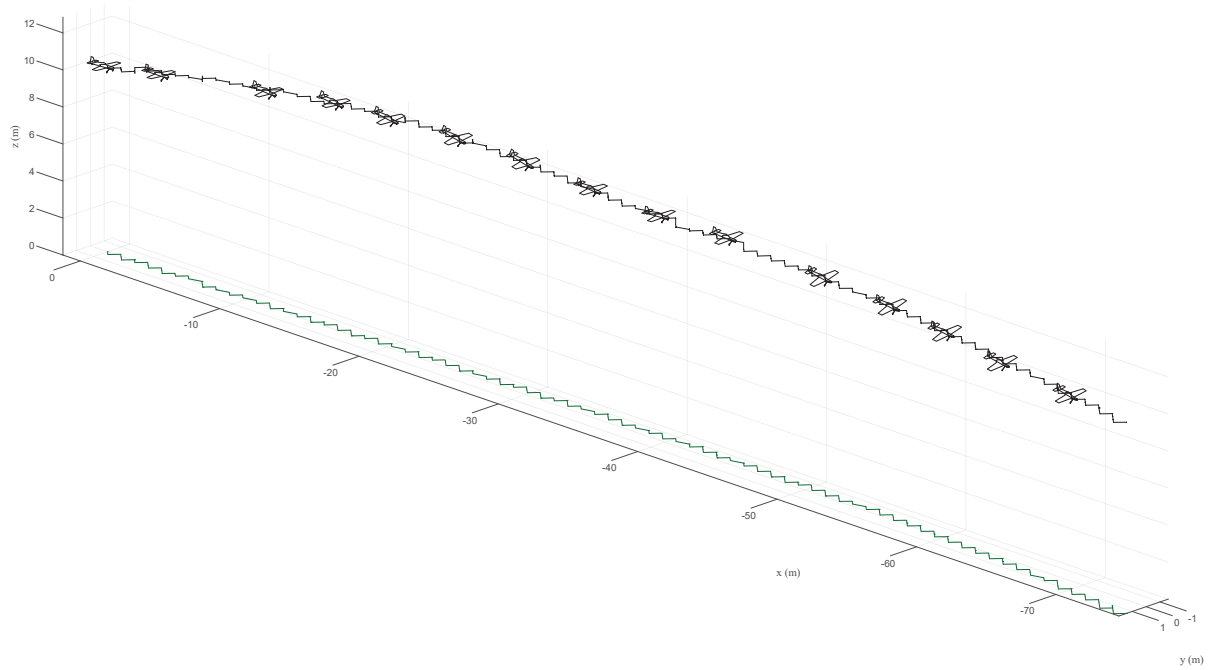

Figure 39: Trajectory plot of the Avistar UAV performing a pitch doublet maneuver using the flight automator (the aircraft is drawn once every 0.2 s).

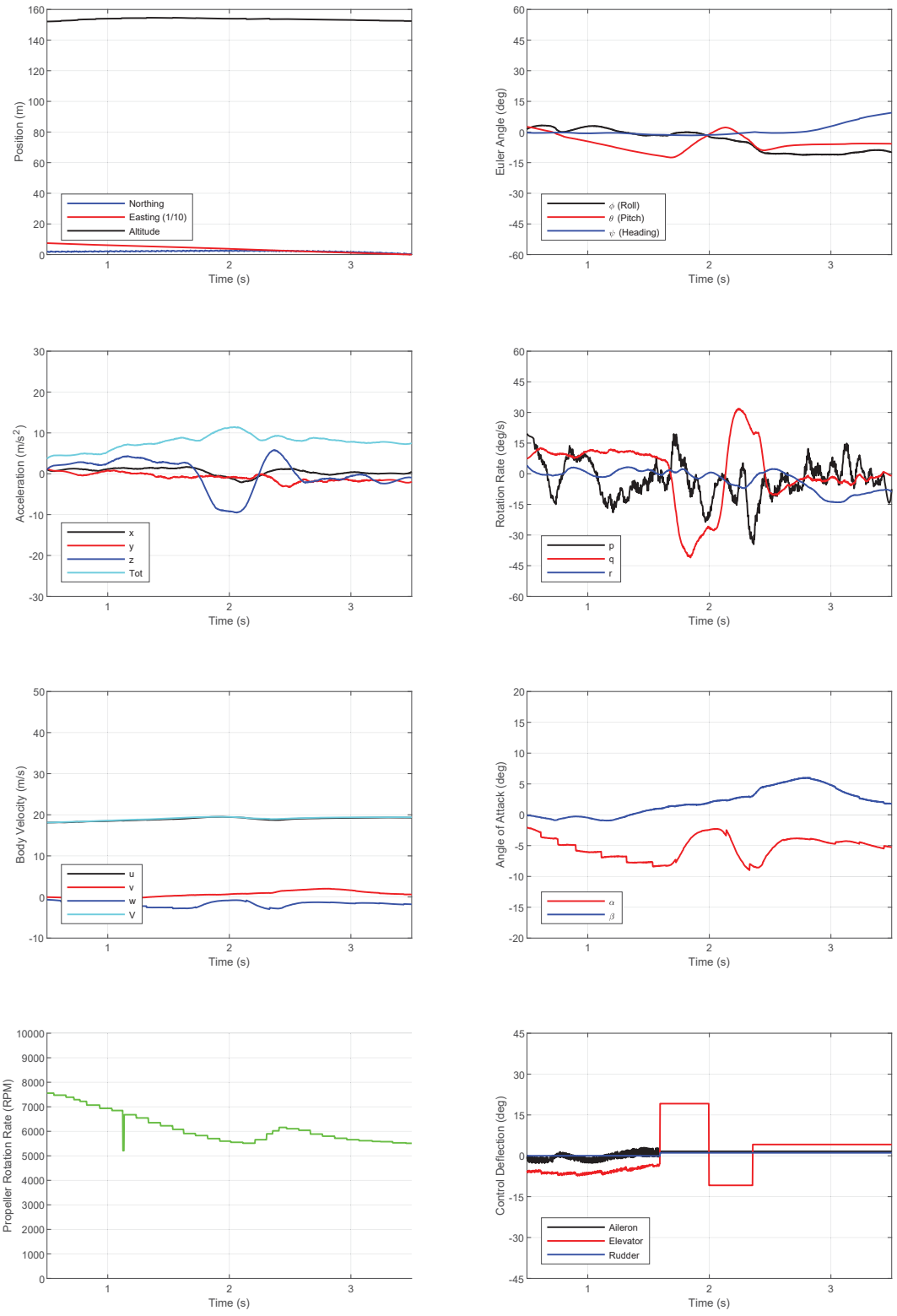

Figure 40: A time history of the Avistar UAV performing a pitch doublet maneuver using the flight automator.

Acknowledgments

The material presented in this paper is based upon work supported by the National Science Foundation (NSF) under grant number CNS-1646383. Marco Caccamo was also supported by an Alexander von Humboldt Professorship endowed by the German Federal Ministry of Education and Research. Any opinions, findings, and conclusions or recommendations expressed in this publication are those of the authors and do not necessarily reflect the views of the NSF.

The authors would like to thank Al Volo LLC for their generous loan of data acquisition equipment and Renato Mancuso for providing integration and flight testing support.

The authors would also like to acknowledge Richard Nai and Mirco Theile for their support during the development and initial testing.

References

[1]Lykins, R. and Keshmiri, S., "Modal Analysis of 1/3-Scale Yak-54 Aircraft Through Simulation and Flight Testing," AIAA Paper 2011-6443, AIAA Atmospheric Flight Mechanics Conference, Portland, Oregon, Aug. 2011.

[2]Johnson, B. and Lind, R., "Characterizing Wing Rock with Variations in Size and Configuration of Vertical Tail," *Journal of Aircraft*, Vol. 47, No. 2, 2010, pp. 567–576.

[3]Perry, J., Mohamed, A., Johnson, B., and Lind, R., "Estimating Angle of Attack and Sideslip Under High Dynamics on Small UAVs," Proceedings of the ION-GNSS Conference, Savannah, Georgia, 2008.

[4]Uhlig, D., Sareen, A., Sukumar, P., Rao, A. H., and Selig, M. S., "Determining Aerodynamic Characteristics of a Micro Air Vehicle Using Motion Tracking," AIAA Paper 2010-8416, AIAA Guidance, Navigation, and Control Conference, Toronto, Ontario, Canada, Aug. 2010.

[5]Dantsker, O. D. and Selig, M. S., "High Angle of Attack Flight of a Subscale Aerobatic Aircraft," AIAA Paper 2015-2568, AIAA Applied Aerodynamics Conference, Dallas, Texas, Jun. 2015.

[6]Mockli, M., *Guidance and Control for Aerobatic Maneuvers of an Unmanned Airplane*, Ph.D. thesis, ETH Zurich, Department of Mechanical and Process Engineering, 2006.

[7]Frank, A., McGrewy, J. S., Valentiz, M., Levinex, D., and How, J. P., "Hover, Transition, and Level Flight Control Design for a Single-Propeller Indoor Airplane," AIAA Paper 2007-6318, AIAA Guidance, Navigation, and Control Conference, Hilton Head, South Carolina, Aug. 2007.

[8]Johnson, E. N., Wu, A. D., Neidhoefer, J. C., Kannan, S. K., and Turbe, M. A., "Test Results of Autonomous Airplane Transitions Between Steady-Level and Hovering Flight," *Journal of Guidance, Control, and Dynamics*, Vol. 31, No. 2, 2008, pp. 358–370.

[9]Gaum, D. R., *Aggressive Flight Control Techniques for a Fixed-Wing Unmanned Aerial Vehicle*, Master's thesis, Stellenbosch University, Department of Electrical and Electronic Engineering, 2009.

[10]Bilodeau, P. R., Poulin, E., Gagnon, E., Wong, F., and Desbiens, A., "Control of a Hovering Mini Fixed Wing Aerial Vehicle," AIAA Paper 2009-5794, AIAA Guidance, Navigation and Control Conference, Chicago, Illinois, Aug. 2009.

[11]Jordan, T. L. and Bailey, R. M., "NASA Langley's AirSTAR Testbed: A Subscale Flight Test Capability for Flight Dynamics and Control System Experiments," AIAA Paper 2008-6660, AIAA Atmospheric Flight Mechanics Conference, Honolulu, Hawaii, Aug. 2008.

[12]Ragheb, A. M., Dantsker, O. D., and Selig, M. S., "Stall/Spin Flight Testing with a Subscale Aerobatic Aircraft," AIAA Paper 2013-2806, AIAA Applied Aerodynamics Conference, San Diego, California, June 2013.

[13]Bunge, R. A., Savino, F. M., and Kroo, I. M., "Approaches to Automatic Stall/Spin Detection Based on Small-Scale UAV Flight Testing," AIAA Paper 2015-2235, AIAA Atmospheric Flight Mechanics Conference, Dallas, Texas, Jun. 2015.

[14]Risch, T., Cosentino, G., Regan, C., Kisska, M., and Princen, N., "X-48B Flight-Test Progress Overview," AIAA Paper 2009-934, AIAA Aerospace Sciences Meeting, Orlando, FL, Jan. 2009.

[15]Lundstrom, D. and Amadori, K., "Raven: A Subscale Radio Controlled Business Jet Demonstrator," International Congress on the Aeronautical Sciences Systems (ICUAS), Anchorage, Alaska, Sep. 2008.

[16]Regan, C. D. and Taylor, B. R., "mAEWing1: Design, Build, Test - Invited," AIAA Paper 2016-1747, AIAA Atmospheric Flight Mechanics Conference, San Diego, California, Jun. 2016.

[17]Regan, C. D., "mAEWing2: Conceptual Design and System Test," AIAA Paper 2017-1391, AIAA Atmospheric Flight Mechanics Conference, Grapevine, Texas, Jun. 2017.

[18]Leong, H. I., Keshmiri, S., and Jager, R., "Evaluation of a COTS Autopilot and Avionics System for UAVs," AIAA Paper 2009-1963, AIAA Infotech@Aerospace, Seattle, Washington, April. 2009.

[19]Esposito, J. F. and Keshmiri, S., "Rapid Hardware Interfacing and Software Development for Embedded Devices Using Simulink," AIAA Paper 2010-3415, AIAA Infotech@Aerospace, Atlanta, Georgia, June 2010.

[20]Garcia, G. and Keshmiri, S., "Integrated Kalman Filter for a Flight Control System with Redundant Measurements," AIAA Paper 2012-2499, AIAA Infotech@Aerospace, Garden Grove, California, June 2012.

[21]Kimberlin, R. D., *Flight Testing of Fixed-Wing Aircraft*, AIAA Education Series, AIAA, Reston, VA, 2003.

[22]Morelli, E. and Klein, V., *Aircraft System Identification: Theory and Practice*, AIAA Education Series, AIAA, Reston, VA, 2006.

[23]Sobron, A., *On Subscale Flight Testing: Applications in Aircraft Conceptual Design*, Ph.D. thesis, Linkoping University, Department of Management and Engineering, Linkoping, Sweden, 2018.

[24]Sobron, A., Lundstrom, D., Larsson, R., Krus, P., and Jouannet, C., "Methods For Efficient Flight Testing And Modelling Of Remotely Piloted Aircraft within Visual Line-of-Sight," International Congress on the Aeronautical Sciences Systems (ICUAS), Belo Horizonte, Brazil, Sep. 2018.

[25]Schulze, P. C., Miller, J. P., Klyde, D. H., Regan, C. D., and Alexandrov, N., "System Identification of a Small UAS in Support of Handling Qualities Evaluations," AIAA Paper 2019-0826, AIAA SciTech Forum, San Diego, California, Jan 2019.

[26]Real Time and Embedded System Laboratory, University of Illinois at Urbana-Champaign, "Solar-Powered Long-Endurance UAV for Real-Time Onboard Data Processing," http://rtsl-edge.cs.illinois.edu/UAV/, Accessed Jan. 2018.

[27]Mirco Theile, "uavAP: A Modular Autopilot for Unmanned Aerial Vehicles," https://github.com/theilem/uavAP, Accessed Apr. 2019.

[28]Laminar Research, "X-Plane 11," http://www.x-plane.com/, Accessed Mar. 2019.

[29]Theile, M., Dantsker, O. D., Nai, R., and Caccamo, M., "uavEE: A Modular, Power-Aware Emulation Environment for Rapid Prototyping and Testing of UAVs," IEEE International Conference on Embedded and Real-Time Computing Systems and Applications, Hakodate, Japan, Aug. 2018.

[30]Mirco Theile, "uavEE: A Modular Emulation Environment for Rapid Development and Testing of Unmanned Aerial Vehicles," https://github.com/theilem/uavEE, Accessed Apr. 2019.

[31]Dantsker, O. D., Ananda, G. K., and Selig, M. S., "GA-USTAR Phase 1: Development and Flight Testing of the Baseline Upset and Stall Research Aircraft," AIAA Paper 2017-4078, AIAA Applied Aerodynamics Conference, Denver, Colorado, June 2017.

[32]Bunge, R. A., Alkurdi, A. E., Alfaris, E., and Kroo, I. M., "In-Flight Measurement of Wing Surface Pressures on a Small-Scale UAV During Stall/Spin Maneuvers," AIAA Paper 2016-3652, AIAA Flight Testing Conference, Washington, D.C., Jun. 2016.

[33]Yu, S., *Flight Maneuver Automation for System Analysis of Small Fixed-Wing UAVs*, Bachelor's thesis, University of Illinois at Urbana-Champaign, Department of Electrical and Computer Engineering, Urbana, IL, 2019.

[34]Mancuso, R., Dantsker, O. D., Caccamo, M., and Selig, M. S., "A Low-Power Architecture for High Frequency Sensor Acquisition in Many-DOF UAVs," Submitted to International Conference on Cyber-Physical Systems, Berlin, Germany, April 2014.

[35]Dantsker, O. D., Mancuso, R., Selig, M. S., and Caccamo, M., "High-Frequency Sensor Data Acquisition System (SDAC) for Flight Control and Aerodynamic Data Collection Research on Small to Mid-Sized UAVs," AIAA Paper 2014-2565, AIAA Applied Aerodynamics Conference, Atlanta, Georgia, June 2014.

[36]Dantsker, O. D., Loius, A. V., Mancuso, R., Caccamo, M., and Selig, M. S., "SDAC-UAS: A Sensor Data Acquisition Unmanned Aerial System for Flight Control and Aerodynamic Data Collection," *AIAA Infotech@Aerospace Conference, Kissimee, Florida, Jan 2015.*.

[37]Dantsker, O. D., Theile, M., and Caccamo, M., "A High-Fidelity, Low-Order Propulsion Power Model for Fixed-Wing Electric Unmanned Aircraft," AIAA Paper 2018-5009, AIAA/IEEE Electric Aircraft Technologies Symposium, Cincinnati, OH, July 2018.

[38]Al Volo LLC, "Al Volo: Flight Systems," http://www.alvolo.us.